

# Oil spill detection from Synthetic Aperture Radar Earth observations: a meta-analysis and comprehensive review

Hamid Jafarzadeh<sup>a</sup>, Masoud Mahdianpari<sup>a,b</sup>, Saeid Homayouni<sup>c</sup>, Fariba Mohammadimanesh<sup>b</sup> and Mohammed Dabboor<sup>d</sup>

<sup>a</sup>Department of Electrical and Computer Engineering, Memorial University of Newfoundland, St. John's, Canada; <sup>b</sup>C-CORE, St. John's, Canada; <sup>c</sup>Institut National de la recherche Scientifique (INRS), Centre Eau Terre Environnement, Québec City, Canada; <sup>d</sup>Science and Technology Branch, Environment and Climate Change Canada, Government of Canada, Dorval, Canada

## ABSTRACT

Oil spills are one of the most hazardous disasters with significant short- and long-term effects on fragile marine ecosystems. Synthetic Aperture Radar (SAR) has been considered an effective technology for mapping and monitoring oil spills in the marine environment, primarily thanks to its weather-, illumination-, and time-independent capabilities. To cope with serious oil spill threats, researchers have developed various analytical methodologies utilizing key advantages of SAR imagery to identify the occurrence of oil spills and discriminate lookalikes. Choosing the appropriate SAR specifications and investigating the effects of field conditions are challenging for oil spill monitoring and should be investigated further. This paper presents a comprehensive review study on maritime surveying and oil slick detection using SAR imagery through indexed research studies' compilation and analysis. To this end, a total of 230 peer-reviewed papers, published in various remote sensing (RS) journals and 78 conference papers in the International Society for Photogrammetry and Remote Sensing (ISPRS) archive and the IEEE International Geoscience and Remote Sensing Symposium (IGARSS) proceedings were reviewed. Our review study represents a meta-analysis investigation of these papers focusing on several features, including data, sensor type, imaging mode, microwave carrier frequency (e.g., L-, C-, and X-bands), polarization option (i.e., single-pol, dual-pol, full-pol, and compact-pol), incidence angle, and wind speed. Furthermore, it provides an overview of the RS techniques developed to deal with the oil spill detection task. This paper can be a guideline for two groups of audiences; those interested in oil spill monitoring who want to get an overview of the problem and how to address it, and those already working in the field who want to understand the scope of the work being accomplished. Consequently, the current paper contributes both to academic RS research and to practical applications.

## KEYWORDS

Marine pollution; oil spills; satellite Earth observations; remote sensing; SAR

## 1. Introduction

Pollution of the oceans and seas from oil spills has long been a significant and unavoidable problem (Fustes et al. 2014; Bayındır, Frost, and Barnes 2018; K Topouzelis *et al.*; Ivanov 2010). Oil spills resulting from intentional or accidental release of liquid petroleum hydrocarbons into water are responsible for several ecological disasters that affect the marine life cycle and damage the quality and productivity of the marine environment (Bayındır, Frost, and Barnes 2018; Salberg, Rudjord, and Schistad Solberg 2014; Singha, Bellerby, and Trieschmann 2012). Because almost two-thirds of the Earth's surface is covered by oceans, contributing to the quality of life and economic livelihood of humans worldwide, protecting marine environments' health is of crucial importance for both short- and long-term sustainability (Lang et al. 2017).

In the marine environment, oil spills are more hazardous and destructive than those on flatter terrain. They can spread rapidly over several hundred kilometers and form a thin crust of oil, which can cover beaches. Detection and monitoring such pollution is a time-consuming and costly task. However, it is crucial to develop an immediate response program to reduce catastrophic effects (Raeisi, Akbarizadeh, and Mahmoudi 2018). A practical operation to reduce the environmental effects of oil pollution depends on the marine environment's systematic monitoring. This operation allows for the accurate estimation of oil spread areas, allowing rapid response and recovery (Keramitsoglou, Cartalis, and Kiranoudis 2006; Dutta et al. 2018). In the last decades, the detection of oil spills over oceans has received considerable attention because they pose threats to human health and have severe environmental and economic impacts on the marine environment, fisheries, wildlife, benthic communities, the

32 human settlement on the beaches, mangrove forests, and other social interests (Anne H. Schistad Solberg 2012;  
33 Zhang et al. 2011; Dabboor et al. 2018; Nunziata et al. 2019).

34 As a result of increasing marine transport trade and developing marine petroleum platforms, the risk for  
35 environmental pollution due to oil discharges has been dramatically increased in the past decades. Therefore, the  
36 marine environment has become an urgent subject of public, political, and scientific concern (Liu et al. 2010; Chang  
37 et al. 2008). The exploration, production, transportation, refining, storage, distribution, and consumption of oil and  
38 petroleum products is overgrowing all over the world; consequently, the threat of destructive and hazardous effects  
39 of oil pollution increases accordingly as oil spills frequently occur in the world's marine water bodies (Caruso et al.  
40 2013; de Oliveira et al. 2020). According to the international literature, the primary sources of oil slicks are  
41 operational/illegal discharges from vessels, platform accidents, and natural resources (Mera et al. 2012; Sharafat  
42 2000). Although there are different sources for oil slicks on sea, ranging from human-made to natural, previous  
43 studies showed that marine tankers, offshore platforms, and large ships are major sources of oil spills in seas or  
44 oceans (Duk-jin Kim, Moon, and Kim 2010; Chen et al. 2019).

45 Monitoring and detecting oil slicks and predicting their trajectories play a crucial role in contingency planning for  
46 oil spills to conserve marine ecosystems and wildlife (Ceyhun 2014; Zhang et al. 2020). In order to make the proper  
47 response to environmental emergencies, effective monitoring and intervention means are required (Shu et al. 2010).  
48 Traditional ocean surveillance systems, including ships and aircrafts equipped with instruments, such as radar  
49 systems, are costly and have limitations for large areas monitoring. Therefore, given the need for near real-time  
50 detection and monitoring of oil spills, remote sensing (RS) satellite data have proven to be a suitable and efficient  
51 option that provides a cost-effective solution to accomplish such a task (Buono et al. 2019; Mera et al. 2014). Satellite  
52 RS systems improve the operational monitoring of Earth's surface by covering broad geographical areas with multi-  
53 sensor and multi-temporal data (Ivanov 2010; Li et al. 2019; Jafarzadeh and Hasanlou 2019b; Mahdianpari et al.  
54 2020; Jafarzadeh and Hasanlou 2019a).

55 In the literature, several survey studies overview the oil spill issues from the RS point of view (e.g., (Fingas and  
56 Brown 2018, 2014; Leifer et al. 2012; Robbe and Hengstermann 2006; Migliaccio,  
57 Nunziata, and Buono 2015; Gens 2008)). These studies are mainly dedicated to characteristics and utilization of  
58 different sensor types, existing techniques for oil spill extraction, and applications. Brekke and Solberg (Brekke and  
59 Solberg 2005b) presented the first review of RS applications in oil spill detection. They provided a general review  
60 focusing on the detectability of oil spills using different sensor types under various conditions.

61 The main systems to monitor sea-based oil pollution are the use of satellites equipped with Synthetic Aperture  
62 Radar (SAR). However, a comprehensive overview and investigation of different SAR sensors' characteristics,  
63 employed SAR-based oil spill detection schemes, extracted and adopted features from SAR data, impacts of  
64 environmental conditions on SAR images, etc., is missing, and would be welcome by those who seek to learn the  
65 principles of using SAR data in oil spill detection. Thus, the current review paper aims to present a comprehensive  
66 and thorough survey of publications to point out the most successful and utilized characteristics of SAR data, plus  
67 reliable and practicable algorithms for oil spill monitoring in marine regions. Across a meta-analysis, we have  
68 recognized, categorized, and analyzed the reviewed literature. To the best of our knowledge, this is the first meta-  
69 analysis, wherein the role of SAR systems is thoroughly discussed for the oil spill detection task.

70 Table 1 summarizes the earlier review papers on oil spill detection using RS data. It should be noted that the  
71 available review papers are descriptive (i.e. discuss the issue of oil spills more generally and from some specific point  
72 of view) and do not convey a quantitative assessment of the oil spill detection task. Accordingly, the main goal of  
73 this study is to fill this knowledge gap by reviewing SAR-based oil spill detection papers (e.g. highlighting most  
74 commonly

**Table 1.** A summary of related surveys on remote sensing oil spill detection (the number of citations is reported by 27 September 2020, on the Web of Science database).

No.	Title	Year	Citation	Publication	Description	Reference
1	A Review of Oil Spill Remote Sensing	2018	46	Sensors	Discusses progress in oil spill sensor development and their capabilities to apply to surveillance to oil discharges monitoring.	(Fingas and Brown 2018)
2	Oil spill detection by imaging radars: Challenges and pitfalls	2017	36	Remote Sensing of Environment	Focuses on discriminating mineral oil films and biogenic slicks. To this end, conventional methods which are widely used for discriminating purposes, critically were reviewed, and some suggestions to improve oil spill detection algorithms were given.	(Alpers, Holt, and Zeng 2017)
3	SAR polarimetry for sea oil slick observation	2015	71	International Journal of Remote Sensing	The more relevant polarimetric SAR-based approaches for sea oil spill detection were discussed. Plus, key characteristics of polarimetric SAR in terms of water-surface oil spill observation were reviewed.	(Migliaccio, Nunziata, and Buono 2015)
4	Review of oil spill remote sensing	2014	211	Marine Pollution Bulletin	The characteristics and capabilities of various measuring devices based on different regions of the electromagnetic spectrum were discussed from oil discharges detection viewpoint.	(Fingas and Brown 2014)
5	State of the art satellite and airborne marine oil spill remote sensing: Application to the BP Deepwater Horizon oil spill	2012	248	Remote Sensing of Environment	This review generally shows the specialized sensors' advantages over other technologies for observing oil spill response.	(Leifer et al. 2012)
6	Oil Spill Detection by SAR Images: Dark Formation Detection, Feature Extraction and Classification Algorithms	2008	149	Sensors	Presents an overview of the methodologies used to distinguish oil spills from other natural phenomena on SAR images. Plus, common methods to detect dark formations on the SAR images, the features which are extracted from candidate oil spill areas and the most used classifiers are also discussed.	(Topouzelis 2008)
7	Oceanographic Applications of SAR Remote Sensing	2008	14	GIScience & Remote Sensing	Provides a review of the use of SAR for oceanographic applications including oil spill detection.	(Gens 2008)
8	Oil spill detection by satellite remote sensing	2005	604	Remote Sensing of Environment	Discusses different satellite based sensors and oil spill detectability under varying conditions. In addition, oil spill detection techniques on a more general level were reviewed.	(Brekke and Solberg 2005)
9	Review of oil spill remote sensing	1997	167	Spill Science & Technology Bulletin	Gives an overview of promising role of RS technologies in oil spill detection.	(Fingas and Brown 1997)

76 investigated study areas, mostly used sensor types, number of images utilized per study, frequently utilized  
77 polarization modes, most popular adopted methods, etc.).

## 78 **2. Background**

79 Marine oil slicks, based on spill sources, can be categorized as two main groups: (1) biogenic oil and (2) mineral oil.  
80 The former, also called surfactants, is surface films that contain surface-active organic compounds produced by  
81 marine plants (e.g., planktons) or animals (e.g., fish) or they are floating macro-algae such as sargassum and kelp  
82 (Najoui et al. 2018; Minchew, Jones, and Holt 2012). The latter contains two subcategories, including natural oil  
83 seeps that stem from sea bottom petroleum reservoirs (crude oil) and anthropogenic oil spills that discharged and  
84 leaked from ships and platforms, oil terminals, processing of industrial or urban plants (e.g., sewage plants), oil  
85 pipelines, and refineries (Najoui et al. 2018; Espedal and Johannessen 2000). It is important to note that the focus  
86 of this paper is to review the studies and advances to address the monitoring of mineral oil spills. So anywhere in  
87 the paper, the phrase “oil spill” refers to anthropogenic oil spills, not any kind of spills.

88 The use of remotely sensed data in the past few decades has been extensively considered for tracking and  
89 detecting oil spills. Both optical and radar satellite Earth observations have been used for this application (Bayramov,  
90 Kada, and Buchroithner 2018; Jha, Levy, and Gao 2008; Xing et al. 2015). However, each option has its own  
91 advantages and disadvantages, which are briefly discussed in the following subsections.

### 92 **2.1. Optical data**

93 With respect to weather conditions, the clear-sky optical imagery is challenging over the seas and oceans; thus, the  
94 use of optical products has not been as widespread as that of SAR data in oil pollution studies. Although the  
95 utilization of optical sensors is severely constrained by sun illumination and cloud-free requirements, integrating  
96 multi-sensor data can be beneficial and to some extent, compensates the limitations of visible sensors (Brekke and  
97 Solberg 2005b). Thanks to temporal resolution and spatial coverage of passive optical sensors, they could provide a  
98 unique complement to fill spatial and temporal gaps for complete coverage of an oil spill (Oscar Garcia-Pineda et al.  
99 2020; Sun et al. 2016; Hu et al. 2009). Moreover, multispectral observations of optical images give additional  
100 information to distinguish actual oil spills from water features (e.g., algal blooms) (Brekke and Solberg 2005b; Zhao  
101 et al. 2014a). In contrast, it would be challenging to discriminate between oil slicks and such features on the SAR  
102 data since they have similar scattering properties (Zhao et al. 2014b; Bayramov, Kada, and Buchroithner 2018).  
103 However, detailed oil spectral properties may not be determined across the visible spectrum, and one could not  
104 categorically identify oil discharges using only optical range (M. Fingas and Brown 2018, 2014).

### 105 **2.2. SAR data**

106 During the past decades, SAR has received considerable attention in RS communities and became an indispensable  
107 source of information in Earth observation, notably because of its broad coverage and almost all-weather and all-  
108 day imaging capabilities under the different environmental conditions at the fine spatial resolution (Arslan 2018;  
109 Bayramov, Kada, and Buchroithner 2018; El-Magd et al. 2020; Akar, Szen, and Kaymakci 2011; Topouzelis et al.  
110 2006). Despite some challenges of utilizing SAR in oil spill detection (as discussed in the following subsection), it has  
111 become a useful and valuable tool for rapid and accurate marine pollution monitoring (Chaudhary and Kumar 2020;  
112 Carvalho et al. 2019). Unlike optical sensors, SAR signal penetration depth through natural media and sensitivity to  
113 surface roughness, altered in an oil spill, helps observe oil pollution (Shahsavahghighi et al. 2013).

114 The primary steps in pre-processing SAR images are divided into four parts: (1) radiometric calibration, (2)  
115 geocoding, (3) filtering, and (4) land masking, and will be described briefly below. First of all, to minimize the  
116 radiometric distortions and confirm that the received signals in SAR data are associated with the sigma naught  
117 backscattering coefficient, which expresses the reflective strength of a radar target, the radiometric calibration is

118 applied (Stussi, Amélie Beaudoin, and Gigord 1996; Frulla et al. 1998). The second step, known as SAR data  
119 geocoding, is essential, ensuring that the image displays the correct location on the Earth's surface. This step also  
120 enables integrating multi-source geospatial data to increase the accuracy of oil pollution monitoring and detection  
121 procedures in SAR data (Moreira et al. 2013; Loew and Mauser 2007). As the third step, speckle removal is crucial in  
122 pre-processing and interpreting SAR data, especially in oil spill monitoring (Shah et al. 2017). The speckle  
123 phenomenon results from the coherent interference of radar echoes from target scatters (Caruso et al. 2013). It  
124 causes a pixel-to-pixel variation of intensities that produces a "salt and pepper" appearance in SAR images (Lee et  
125 al. 1994; McCandless and Jackson 2004). The presence of SAR speckle-noise reduces the quality of images and  
126 degrades the separability between the oil spill candidate areas and the background, which seriously affects oil slicks'  
127 detection (Xu et al. 2015; Wang, Zhang, and Patel 2017; Chierchia et al. 2017).

128 In the reviewed literature, the following filters were employed to minimize the effects of speckle-noise and avoid  
129 producing false detections: Lee (Dutta et al. 2018; Chaudhary and Kumar 2020; Bayramov, Kada, and Buchroithner  
130 2018; Misra and Balaji 2017; Tong et al. 2019; Song et al. 2018; Li, Jia, and Velotto 2016a), enhanced Lee (Zhang et  
131 al. 2020; Li et al. 2018), Frost (Carvalho et al. 2016), Gaussian (Shu et al. 2010; Song et al. 2018), sigma (Barni, Betti,  
132 and Mecocci 1995), Kuan (Barni, Betti, and Mecocci 1995), median (Lang et al. 2017; Cantorna et al. 2019; Konik and  
133 Bradtke 2016; Sefah-Twerefour, Wiafe, and Adu Agyekum 2012; Chang, Cheng, and Tang 2005), Gamma (Arslan  
134 2018; Martinis, Gähler, and Twele 2012), Lopez (Li et al. 2018), boxcar (Guo, Wei, and Jubai 2018; Hassani, Sahebi,  
135 and Asiyabi 2020; Li et al. 2018; Espeseth et al. 2017; Yin, Moon, and Yang 2015), and non-local mean filters (Lang  
136 et al. 2017). Finally, land masking is a further step in the pre-processing of SAR images that contain land surfaces.  
137 This step prevents interfering of the land pixels with the detection of oil spills (Singha, Vespe, and Trieschmann  
138 2013).

### 139 **2.3. Challenges of utilizing SAR data**

140 Oil spill detection in seawater is clarified by comparing oil spectral radiance and surrounding water radiance (Araújo  
141 et al. 2004). Owing to the influence of short-wavelength gravity waves (produced on local winds and are responsible  
142 for the sea spectrum energy spreading) and capillary waves (engendered by friction and associated with wind speed  
143 and sea- surface characteristics), backscattering from the sea surface is weakened, resulting in oil slicks to appear  
144 as dark spots with complex patterns on SAR images (Guo, Wei, and Jubai 2018; Mercier and Girard-  
145 Arduhin 2005; Arslan 2018; Li et al. 2013; Arduhin, Mercier, and Garello 2003; Grégoire Mercier and Arduhin 2006a;  
146 Minchew, Jones, and Holt 2012). These wind-generated waves are called "Bragg waves" (Velotto, Soccorsi, and  
147 Lehner 2014) and are directly related to the radar brightness of the sea (Perkovic et al. 2010; Shao, Sheng, and Sun  
148 2017).

149 No Bragg waves are generated at very low wind speeds, causing the entire image to be dark due to specular  
150 reflection of the radar signal and rendering any slick invisible (Perkovic et al. 2010; Alpers et al. 2013). Consequently,  
151 identification of oil spills in SAR images always includes the first and essential step, which is detecting any dark-  
152 spotted areas that have high contrast relative to its surrounding (Zhang et al. 2008; Akkartal and Sunar 2008).  
153 Unluckily, several ocean phenomena and interfering substances can dampen the Bragg waves and produce low  
154 backscattering areas. They appear as dark patches (false targets) in SAR imagery, which are called lookalikes (Najoui  
155 et al. 2018).

156 In general, based on a comprehensive literature review, main types of oil spill lookalikes that frequently appear  
157 on SAR imagery are presented in Figure 1 (Espedal and Johannessen 2000; Holstein et al. 2018; Vijayakumar and  
158 Rukmini 2016; Carvalho et al. 2020; Chaturvedi, Banerjee, and Lele 2020; Topouzelis et al. 2007; Fingas and Brown  
159 2018; Clemente-Colon and Yan 2000; Alpers, Holt, and Zeng 2017). A short description of each of these categories  
160 is reported in the following:

- 161 (1) Natural biogenic slicks: as discussed earlier, these are surface films produced by the decaying of marine  
162 organisms. This category is the most intricate oil spill lookalike because radar signatures of biogenic spills can

163 be quite similar to those of mineral oil films (Skrunes, Brekke, and Eltoft 2014; Alpers, Holt, and Zeng 2017).  
 164 Since the only oil spills considered in this paper are anthropogenic ones, the natural biogenic slicks are  
 165 grouped as lookalikes.  
 166 (2) Low wind zones: the surface roughness strongly depends on the wind, and variability in wind speed changes

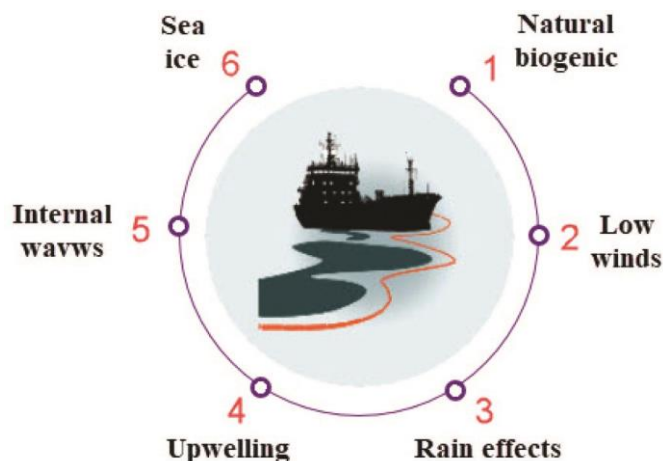


Figure 1. Main types of oil spill lookalikes that frequently appear on SAR images.

167 the backscatter level. Low wind speed (i.e., wind speed <3 m/s) produces a low backscatter area because of  
 168 atmospheric circulation variation. Coastal topography and man-made obstacles also cause wind shadowing  
 169 and produce dark patches (Clemente-Colon and Yan 2000).  
 170 (3) Rain effects: the atmospheric attenuation due to volume scattering in a rain system also produces a low  
 171 backscatter area (Clemente-Colon and Yan 2000). This is problematic at higher frequencies (Danklmayer et  
 172 al. 2009). Furthermore, rain cells hit the sea surface, resulting in turbulence in the upper water layer and  
 173 dampen the Bragg waves.  
 174 (4) Upwelling: cold and nutrient-rich water reaches the surface through an oceanographic phenomenon known  
 175 as upwelling. A decrease of water temperature on the sea surface alters the stability of the air–sea interface,  
 176 results in lower wind stress, and reduces Bragg waves. Furthermore, the nutrient-rich waters on the water  
 177 surface contribute to the formation of natural biogenic slicks (Clemente-Colon and Yan 2000).  
 178 (5) Internal waves: they affect the local sea surface velocities, cause divergent flow regimes, and alter the Bragg  
 179 spectrum. Tidal flow over underwater sand banks also has a similar effect. The internal ocean waves are  
 180 generated when the water density changes with depth, and strong currents interact with shallow underwater  
 181 bottom topography. The SAR image of internal waves consists of adjacent bright and dark bands (Clemente-  
 182 Colon and Yan 2000;  
 183 Solberg, Brekke, and Husoy 2007).  
 184 (6) Sea ice: first-year ice floes have a smooth surface and high salinity. Accordingly, they reflect the SAR signal  
 185 and appear dark relative to multiyear ice in SAR imagery. Similarly, grease ice (i.e., newly formed ice  
 186 composed of small millimeter-sized crystals) also dampens the Bragg waves and reduces SAR backscatter.  
 187 Grease ice forms slicks, similar to those produced by mineral or biogenic surfactants (Clemente- Colon and  
 188 Yan 2000).  
 189 (7) Other sources: these include dry-fallen sand banks during ebb tide, storm water that flows from land into the  
 190 sea, plant oil spilled into the sea during tank cleaning of ships, transporting palm oil, fish oil, fluvial run-off,  
 191 ship wakes, and coastal boating (Alpers, Holt, and Zeng 2017).

192 Distinguishing oil spills from lookalikes is a challenging and complex issue, which involves analysis of surface oil  
 193 characteristics in the SAR images (e.g., shape, size, dB-values, gradients, and texture), environmental conditions  
 194 (e.g., instantaneous wind and currents), and oil-spill prone areas (e.g., locations of oil platforms, ship lanes, and

195 natural seepage) (Espedal 1999; Arduin, Mercier, and Garello 2003; Akar, Szen, and Kaymakci 2011). Hence,  
196 choosing the appropriate SAR specifications and investigating the effects of field conditions is challenging for the oil  
197 spill monitoring task and should be explored more thoroughly.

198 The knowledge of wind conditions is necessary for oil spill monitoring. The detection of an oil spill is strongly  
199 dependent upon the wind speed. Many research studies investigated the relation between SAR backscatter and  
200 wind conditions in marine applications (Skrunes et al. 2018; Dagestad et al. 2013). The wind is the component that  
201 causes waves and can significantly impact oil's behavior on the ocean surface and disrupt data analysis, notably at  
202 high and very low wind speeds (Fingas 2011; Skrunes et al. 2018). Subsequently, the visibility of oil slicks is restricted  
203 to a limited range of wind speeds (Fan et al. 2015).

204 In addition to wind conditions, the detectability of oil spills in SAR data is a function of the sensor characteristics.  
205 Frequency is of the most fundamental characteristics of SAR imaging that encompasses the different microwave  
206 bands used in data acquisition, including L-, C- and X-bands. Notably, for L-, C-, and X-band SAR, the detectability  
207 relies on polarization, noise equivalent sigma zero (NESZ), incidence angle, swath width, and spatial resolution  
208 (Ivonin et al. 2020; Skrunes, Brekke, and Eltoft 2014; Cheng et al. 2011; Latini, Fabio, and Jones 2016).

209 One of the critical factors affecting surface backscattering and, consequently, oil spill characterization is the NESZ,  
210 i.e., the noise equivalent sigma zero, which measures the sensitivity of a SAR sensor. The NESZ value must be lower  
211 than the measured normalized radar cross-section (NRCS) value so that the backscattered signal from the surface  
212 will not be corrupted by noise (Skrunes, Brekke, and Eltoft 2014; Alpers, Holt, and Zeng 2017; Angelliaume et al.  
213 2018). The NESZ and radar incidence angle have an inverse variation relationship. The increase in the radar incidence  
214 angle leads to a decrease in SAR backscattering intensity. As the backscatter decreases, the signal approaches the  
215 NESZ; therefore, causing the detection to be challenging (Skrunes et al. 2018; Marghany 2016).

216 Other critical elements of SAR to be considered are the swath width and the spatial resolution, which refers to  
217 the smallest discernible details on images. There is an inverse relationship between these two parameters. It makes  
218 sense to choose large swath widths for operational oil spill detection because it covers and observes large areas,  
219 although very small oil slicks will not be detected (Topouzelis 2008).

220 **3. Methods**

221 **3.1. Bibliographic base and search query**

222 To prepare for this meta-analysis and comprehensive review, the Institute for Scientific Information (ISI) Web of  
223 Science and Scopus bibliographic databases were used on and up to 27 September 2020, for full- length English  
224 language papers, including journal articles and conference papers constrained to a time from 1990 to 2020. To this  
225 end, a logical literature search query was systematically developed using four sets of keywords to locate highly  
226 relevant papers in the database (see Figure 2). In order to retrieve papers that utilized SAR RS data and addressed  
227 the application of detection in the marine area, the keywords in the second, third and last columns were searched  
228 in the topic field (title/abstract/keyword). However, the first column keywords were exclusively searched in the title  
229 field to narrow the search down and make it more specific. This research obtained only the studies that analyzed  
230 the SAR data for anthropogenic oil spill detection.

231 Based on the search query, 1396 journal and conference papers were found in the mentioned databases.  
232 Afterward, we followed the methodology of Preferred Reporting Items for Systematic Reviews and Meta-Analyses,  
233 known as PRISMA (Moher et al. 2009) to select eligible papers to be included in our analysis. PRISMA is a checklist  
234 designed to improve the reporting standards of systematic literature reviews and meta-analyses. This reporting  
235 guideline consists of four phases flow diagram, including “identification,” “screening,” “eligibility,” and “included”  
236 (see Figure 3).

237 Following an initial assessment of the obtained 1396 published papers, a total of 1061 papers are selected. To be  
238 more specific, only those publications with titles and abstracts related to “oil spill detection by SAR imagery” were  
239 selected for further analysis in the next step. Moreover, only the publications that employed RS techniques based  
240 on airborne or spaceborne SAR data were selected as final items to be reviewed to maintain a controllable workload.  
241 Studies classified as review papers, book chapters, and reports were not considered in this systematic review. From  
242 the conference papers, we selected only those published in the International Society for Photogrammetry and  
243 Remote Sensing (ISPRS) archive and the IEEE International Geoscience and Remote

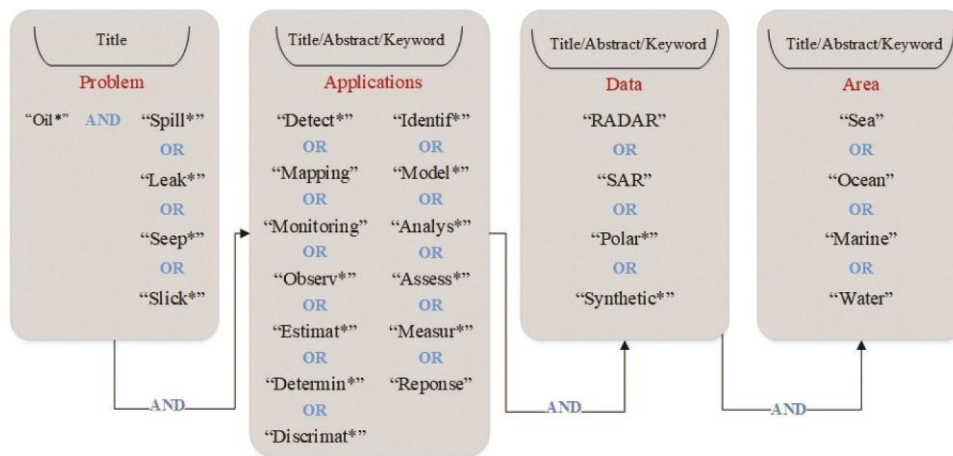
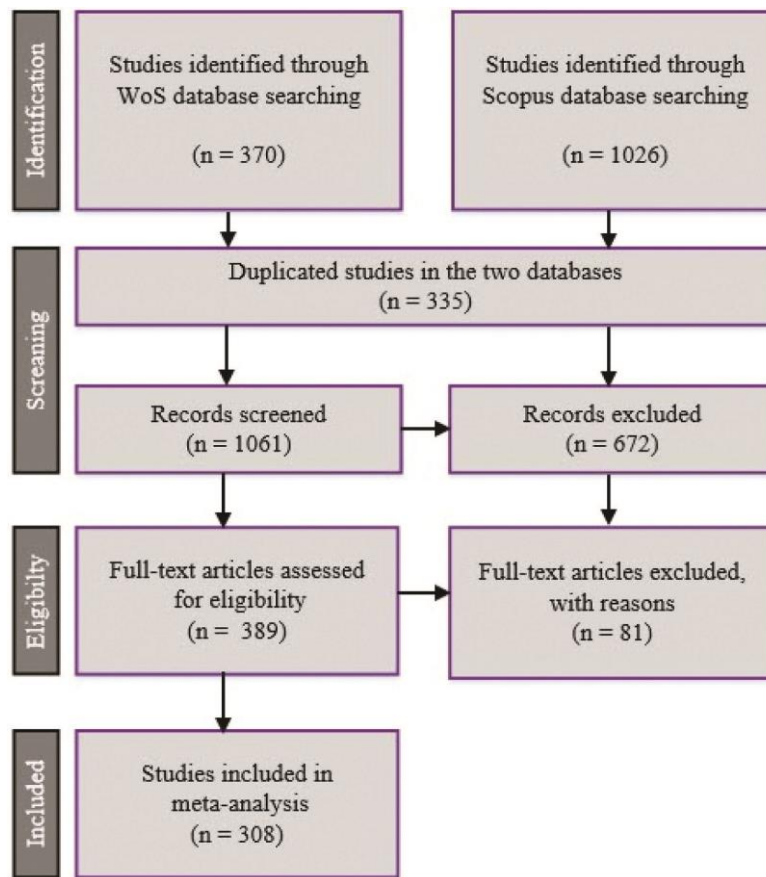


**Figure 2.** Search query criteria design for retrieving literature on SAR-based oil spill detection from WoS and Scopus databases.



244

245 **Figure 3.** PRISMA flow diagram for manuscript selection.

246 **Table 2.** List of extracted attributes from the reviewed papers in the  
247 database.

No.	Attribute	Type	Categories
1	Publication Title	Free text	–
2	Authors	Free text	–
3	Affiliation	Free text	–
4	Publication Year	Free text	–
5	Document Type	Classes	Article; Conference
6	Journal	Free text	–
7	Citation	Numeric	–
8	Study Area	Free text	–
9	Sensor type	Classes	ERS-1,2, JERS-1, RADARSAT-1&2, ENVISAT ASAR, ALOS-1&2 PALSAR, TerraSAR-X, Cosmo Skymed, RISAT-1, Sentinel-1
10	Date of Data Acquisition	Numeric	–
11	Number of images	Numeric	–
12	Platform	Classes	Spaceborne; Airborne
13	Polarization Mode	Classes	Single; Dual; Full; Hybrid
14	Imaging Mode	Free text	–
15	Used frequency	Classes	L; C; X bands
16	Incident Angle	Numeric	Range of incidence angles
17	Wind Speed	Numeric	Range of wind speeds
18	Method	Classes	Classification, Segmentation, Statistical, Deep Learning
19	Research Objective	Free text	–
20	Accuracy Assessment	Numeric	Percentage

248

249 Sensing Symposium (IEEE-IGARSS) proceedings. In addition, papers that did not contain most of the defining features  
250 listed in Table 2 were excluded. Conclusively, 308 papers were identified as eligible for our comprehensive review.  
251 A summary of manuscript selection can be seen in Figure 3.

### 252 **3.2. *Extracted attributes from the screened records***

253 Table 2 includes the extracted attributes from the reviewed studies. This meta-analysis summarized these attributes  
254 to give an overview of how SAR data have been used across studies. Among these attributes, sensor type plays a  
255 crucial role in the SAR specifications, including frequency, incidence angle, and polarization. Another essential  
256 attribute is the type of Earth observation platform; airborne or spaceborne. Since airborne platforms (e.g., UAVSAR)  
257 provide lower spatial coverage than spaceborne sensors, they can be used for close analysis of relatively small case  
258 studies. On the other hand, spaceborne platforms cover a wide ground range with frequent revisit times.

## 259 **4. Results**

260 As mentioned earlier, based on the criteria outlined in the previous section, a total of 308 articles were selected.  
261 Several data categories have been extracted based on the review of journal and conference papers related to oil  
262 spill detection. In this section, detailed results of the systematic review will be presented. To this end, first, the  
263 articles' general characteristics, including the journals, the number of published papers per year, and the study  
264 areas, are presented. Afterward, study regions, SAR sensor types used in the literature and their characteristics such  
265 as frequency and polarization mode, the number of images utilized per study, and different types of methods  
266 employed in oil spill detection were discussed in detail. Finally, the reported accuracies in studies that used different  
267 types of SAR polarizations were assessed. Quantitative and qualitative results of the current meta-analysis are  
268 presented in the remainder of this section.

269 **4.1. General characteristics in oil spill detection studies**

270 Figure 4 indicates the publication trends among 308 papers reviewed using PRISMA and illustrates the number of  
271 major oil spill events within the period 1990–2020. The increasing trend of publications in Figure 4 emphasizes the  
272 importance of oil spill detection for the scientific community. Given the increasing number of SAR sensors and their  
273 promising performance in oil spill detection, about 42% of the papers were published in recent years (2016–2020).  
274 The fact that 42% of the papers were published between 2016 and 2020 could also be related to the European Space  
275 Agency’s open data policy (ESA) adopted for Sentinel- 1 data, making it easier to access SAR data. According to  
276 reports published by (ITOPF 2020), there has been a marked downward trend in the number of oil spill events over  
277 the last few decades. The frequency of oil spills greater than 700 tonnes has been shown in Figure 4.

278 Overall, the reviewed papers in our study were published in 89 different journals and two conferences, revealing  
279 the wide breadth of disciplines interested in the oil spill monitoring theme. We found that 70 of these journals have  
280 published only one or two papers in the field of oil spill detection. Only journals and conferences published more  
281 than two oil spill papers are included in Figure 5.

282 As shown in Figure 5, the highest number (top seven) of publications associated with oil spill detection occurs in

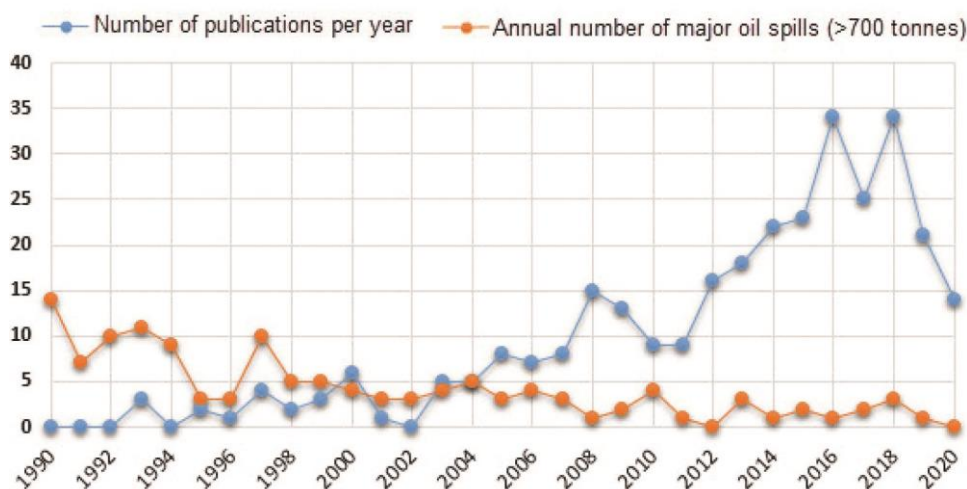
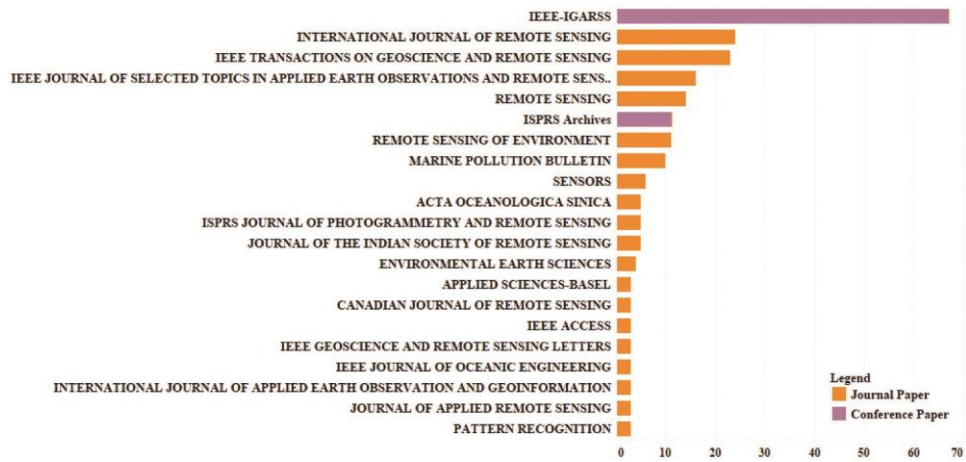


**Figure 4.** The fluctuation and the total number of publications per year, and the annual number of major oil spills from 1990 to 2020.

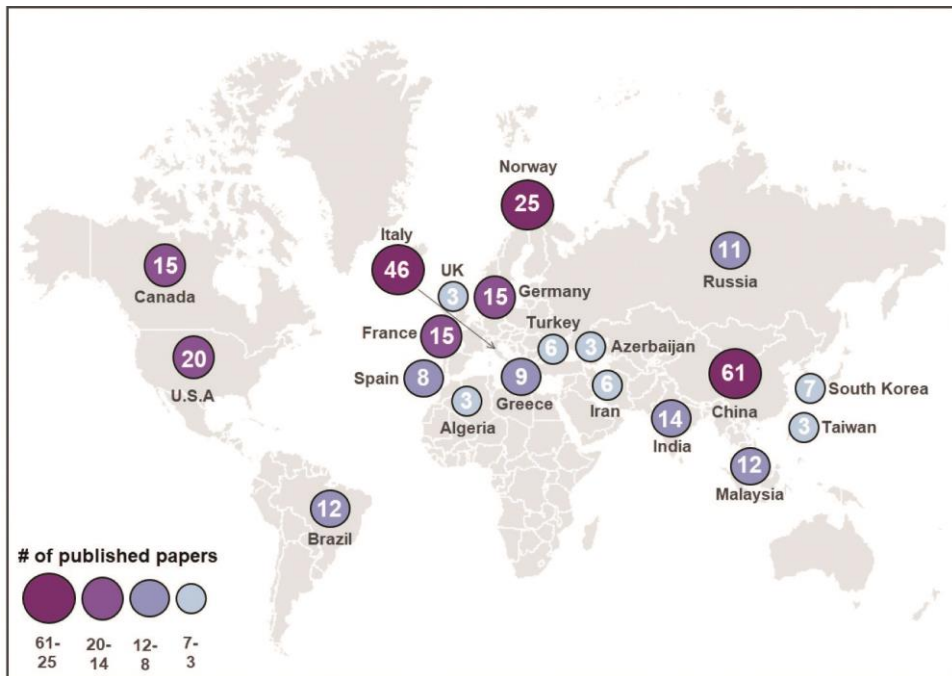
283 the IEEE-IGARSS archive, International Journal of Remote Sensing (IJRS), IEEE Transactions on Geoscience and  
284 Remote Sensing (IEEE-TGRS), IEEE Journal Selected Topics in Applied Earth Observation and Remote Sensing (IEEE-  
285 JSTARS), Remote Sensing (MDPI), ISPRS archives, and Remote Sensing of Environment (RSE).

286 Figure 6 illustrates the published papers’ global geographical coverage based on the articles’ reported research  
287 institutions. In 20 countries, three or more papers were published. As illustrated, researchers affiliated with  
288 institutions in China account for the bulk of oil spill studies with 61 articles, followed by 46 articles in Italy. The  
289 articles from China and Italy consisted of about 34% of the studies. This number of publications may be due to the  
290 universities’ and



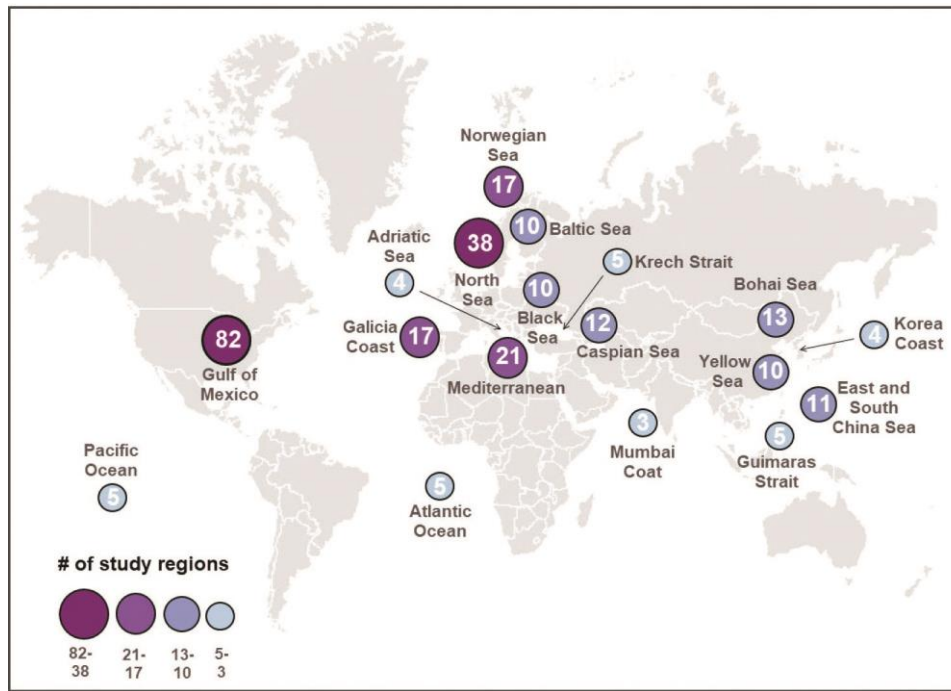
291

292 **Figure 5.** The number of oil spill detection papers published per journal (only those journals published three or more papers  
 293 are included).



294

295 **Figure 6.** Distribution and frequency of published papers per country, according to the country reported in the papers.



296

297 **Figure 7.** The global distribution and counts of study regions from all reviewed oil spill studies.  
 298 institutions' extensive scientific studies located in these countries. It could also be a result of the higher interests in  
 299 marine pollution monitoring in these countries. The remaining countries in which more than three oil spill studies  
 300 have been published are Norway (25), USA (20), Canada (15), France (15), Germany (15), India (14), Brazil (12),  
 301 Malaysia (12), Russia (11), Greece (9), Spain  
 302 (8), South Korea (7), Iran (6), Turkey (6), Algeria (3), Azerbaijan (3), Taiwan (3), and United Kingdom (3).

303 **4.2. Study regions and oil spill-prone areas**

304 The worldwide distribution of study regions is shown in Figure 7. As shown, most studies were conducted in the Gulf  
 305 of Mexico (82). Furthermore, the 38 and 21 studies performed over the North Sea and the Mediterranean Sea  
 306 represent the strong attention of researchers on those areas. Moreover, the number of remaining study areas that  
 307 were studied three or more times in the reviewed literature are as follows: Galicia coast (17), Norwegian Sea (17),  
 308 Bohai Sea (13), Caspian Sea (12), East and South China Sea (11), Baltic Sea (10), Black Sea (10), Yellow Sea (10),  
 309 Atlantic Ocean (5), Pacific ocean (5), Guimaras Strait (5), Kerch Strait (5), Adriatic Sea (4), South Korea coast (4), and  
 310 the coast of Mumbai (3).

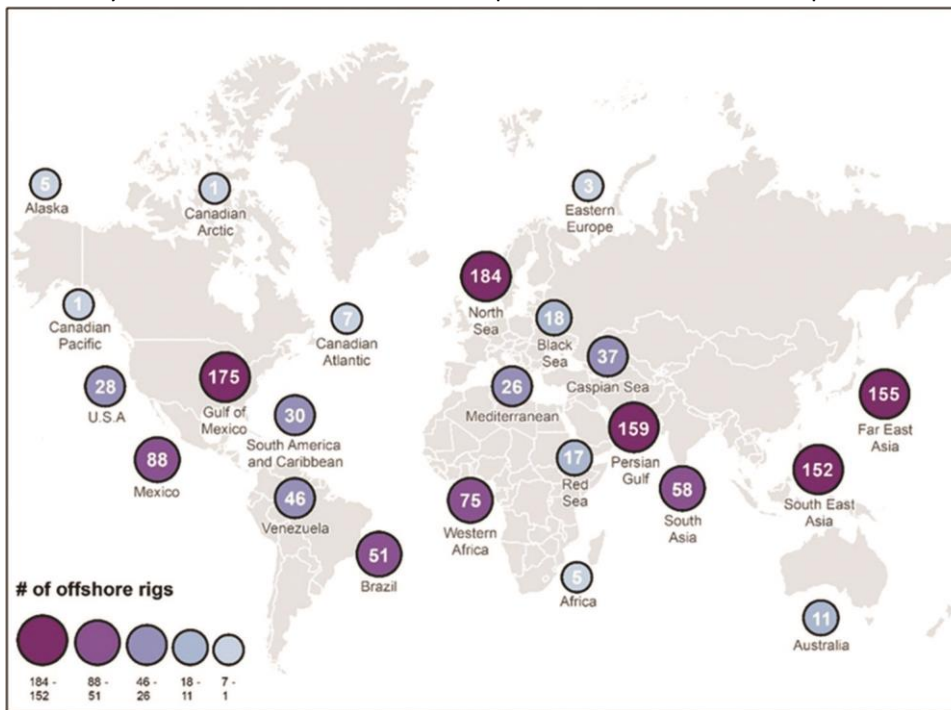
311 Sea-based offshore platforms can be the primary source of marine oil pollution. An offshore oil and gas platform  
 312 includes facilities to explore, extract, store, and process petroleum and natural gas through drilled wells, increasing  
 313 the risk of oil spills ruining and poses devastating effects on the marine environment. As seen in Figure 8, the North  
 314 Sea and the Gulf of Mexico (United States) can be classified as the most prone oil spill zones because of the large  
 315 number of installed offshore drilling rigs, totaling 184 and 175 rigs, respectively (Fazeres-Ferradosa et al. 2019). In  
 316 addition, the significant number of oil platforms in the Persian Gulf (159), far east Asia (155), and southeast Asia  
 317 (152) may also contribute and pose a threat to the marine environment.

318 Accidents involving ships or oil rigs and platforms, breaking of outdated and damaged facilities, human mistakes,  
 319 and wars make the ocean water became contaminated by liquid petroleum hydrocarbon, which would cause  
 320 damages to the marine environment for decades. In some cases, a vast range of polluted marine environment with  
 321 a massive release of tens of millions of oil gallons, resulting in substantial effects from injured wildlife to the loss in

322 tourism revenue. Examples of historical major oil spills are listed in Table 3 (Hoffman and Devereaux Jennings 2011;  
 323 O'Rourke and Connolly 2003; Congress 1991; Chen et al. 2019).

324 **4.3. SAR sensors used for oil spill detection**

325 In the current meta-analysis, satellite-borne SAR has been proven as a useful and indispensable source of



326

327 **Figure 8.** Location and distribution of offshore oil rigs worldwide.

328 **Table 3.** Major oil spill disasters in the world history ranked by the amount of spill  
 329 size.

No.	Spill/Tanker	Location	Date	Amount Spilled (million gallons)
1	Gulf War oil spill	Persian Gulf, Kuwait	19 January 1991	380–520
2	Deepwater Horizon	Macondo Prospect, Central Gulf of Mexico	22 April 2010	206
3	Ixtoc-I Oil Spill	Bay of Campeche off Ciudad del Carmen, Mexico	3 June 1979	140
4	Atlantic Empress Oil Spill	Off the coast of Trinidad and Tobago	19 July 1979	90
5	Kolva River Oil Spill	Kolva River, Russia	6 August 1983	84
6	Nowruz Oil Field Spill	Persian Gulf, Iran	10 February 1983	80
7	Castillo de Bellver Oil Spill	Off Saldanha Bay, South Africa	6 August 1983	79
8	Amoco Cadiz Oil Spill	Portsall, France	16 March 1978	69
9	ABT Summer Oil Spill	About 700 nautical miles off the coast of Angola	28 May 1991	51–81
10	M/T Haven Tanker Oil Spill	Genoa, Italy	11 April 1991	45
11	Odyssey Oil Spill	Off the coast of Nova Scotia, Canada	10 November 1988	40.7
12	The Sea Star Oil Spill	Gulf of Oman	19 December 1972	35.3
13	The Torrey Canyon Oil Spill	Scilly Isles, U.K.	18 March 1967	25–36
14	Sanchi	Off Shanghai, China	6 January 2018	34
15	Irenes Serenade	Navarino Bay, Greece	23 February 1980	30
16	Urquiola	La Coruna, Spain	12 May 1976	30
17	Hawaiian Patriot	300 nautical miles of Honolulu	23 February 1977	30
18	Independenta	Bosphorus, Turkey	15 November 1979	28.9
19	Jakob Maersk	Oporto, Portugal	25 January 1975	26.4
20	Braer	Shetland Islands, UK	5 January 1993	25.5

330

331 data for oil spill detection. Table 4 lists some of the well-known SAR-equipped satellite missions widely employed in  
332 the reviewed literature along with their life span, repeat cycle, wavelength, frequency, polarization, and orbital  
333 inclination.

334 From the RS platform viewpoint, 291 publications have applied satellite-borne SAR images. Sensor types included  
335 in these studies are shown in Figure 9. As shown, ENVISAT, RADARSAT-2, and ERS-2 are the most frequently  
336 employed data sources and were used in 84, 82, and 69 studies, respectively. Moreover, the number of remaining  
337 types of SAR sensors studied oil spill detection are as follows: ERS-1 (52), RADARSAT-1 (45), TerraSAR-X (40), ALOS-  
338 PALSAR (29), UAVSAR (20), COSMO-SkyMed (20), SIR-C/X-SAR (14), Sentinel 1A/ B (13), RISAT-1 (5). Note that  
339 sensors used five times or more in the literature are included in Figure 9.

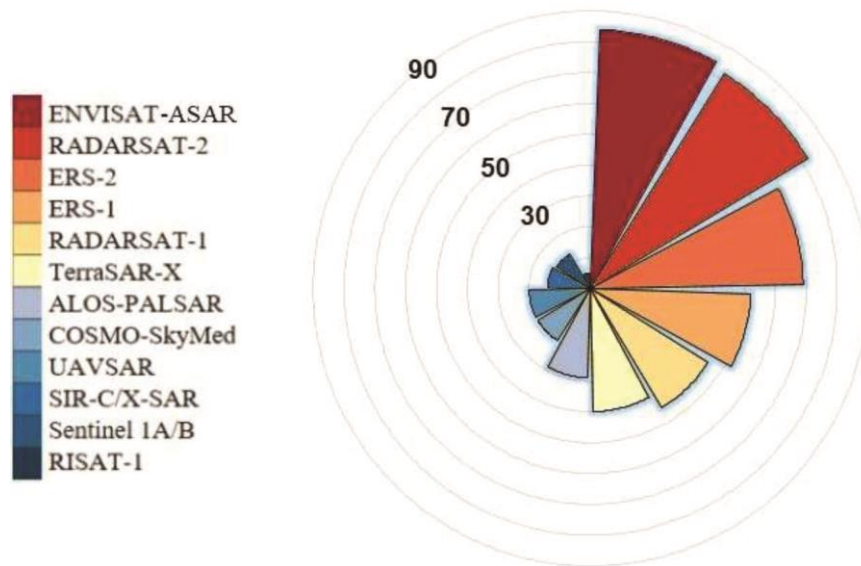
340 Figure 10(a and b) indicates that about 93% of papers used spaceborne SAR data, and the remaining 7% applied  
341 airborne SAR data in oil spill studies. The satellite broad coverage capabilities should be the primary motivation that  
342 most reviewed studies employed spaceborne data sets. The presence of oil spills may appear differently when  
343 different SAR imaging sensors are used because surface characteristics can vary based on wavelength, frequency,  
344 polarization, and incidence angle. SAR sensors operate at different frequencies. Based on the reviewed literature, L-  
345 , C-, and X-band at a wavelength of 24, 6, and 3 centimeters, respectively, are the most used microwave bands for  
346 oil spill monitoring.

347 Regarding the choice of sensor, the reliability of detection is mainly subject to the frequency band and the sensor  
348 noise floor. Gade *et al.* in (Gade et al. 1998) proved that SAR images acquired at high frequency (i.e., X-band or C-  
349 band) are preferable to those acquired at a lower frequency (i.e., L-band) for oil slick detection. The damping ratio  
350 – a measure of the difference in spectral energy density of the ocean surface waves between oil-free and oil-covered  
351 surfaces (Wismann et al. 1998) – increases at higher frequencies, so the contrast between oil spills and clean sea is  
352 reported to be highest in X-band, moderate in C-band, and lowest in L-band (Marzialetti and Laneve 2016; Fingas  
353 and Brown 2018; Skrunes et al. 2015), and that is why X and C-band is superior to L-band (Vespe and Greidanus  
354 2012; Marzialetti and Laneve 2016). However, it is also demonstrated in (Minchew, Jones, and Holt 2012b) that low  
355 noise L-band SAR systems can provide helpful oil spill data and identify oil slick successfully.

356 As shown in Figure 10(a), C-band appears to be the primary SAR wavelength for oil spill detection with 236 studies,  
357 followed by X-band (48 studies) and L-band (31 studies). This fact could be triggered by the higher number of SAR  
358 satellites operating in the C-band than the X- and L-bands (refer to Table 4). According to Figure 10(b), L-band  
359 airborne SAR data has been used in 25 studies in the reviewed literature. Some studies employed a multi-frequency  
360 dataset

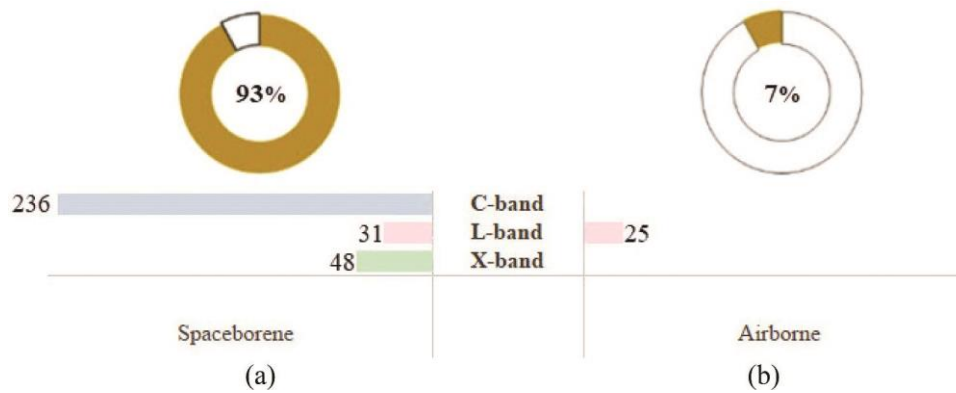
**Table 4.** Characteristics of well-known SAR-equipped satellite missions utilized in the oil spill detection community. The columns “WL,” “Pol” and “OI” indicate wavelength, polarization and orbital inclination, respectively.

Satellite Mission (Sensor)	Life Span	Repeat Cycle (days)	WL (cm)/Band	Pol.	OI (deg.)	Ref.
ERS-1	1991–2000	35, 3, 168	5.66/C-band	Single-VV	98.52	(Singha, Bellerby, and Trieschmann 2012; Bayramov, Kada, and Buchroithner 2018; Chehresa et al. 2016)
JERS-1	1992–1998	44	23.5/L-band	Single-HH	97.7	(Garcia-Pineda et al. 2020; MacDonald et al. 2015)
SIR-C/X-SAR	1994–1994	1	23.5, 5.8 /L-C-band 3.1/X-band	Quad Single-HH	57	(Zhang et al. 2020; Yin et al. 2020; Zheng et al. 2017; Bandiera, Masciullo, and Ricci 2014)
ERS-2	1995–2011	35	5.66/C-band	Single-VV	98.52	(Liu et al. 2010; Chehresa et al. 2016; Garcia-Pineda et al. 2017; Asl et al. 2017)
RADARSAT-1	1995–2013	24	5.66/C-band	Single-HH	98.6	(Bayramov, Kada, and Buchroithner 2018; Cao, Linlin, and Clausi 2017; Xu, Jonathan, and Brenning 2014; Dabboor et al. 2019)
ENVISAT (ASAR)	2002–2012	35	5.63/C-band	Dual	98.55	(Mera et al. 2012; Mera et al. 2014; Bayramov, Kada, and Buchroithner 2018; Wang et al. 2015; Akar, Süzen, and Kaymakci 2011)
ALOS (PALSAR)	2006–2011	46	23.6/L-band	Quad	98.16	(Ozkan et al. 2012; Cheng et al. 2011; Wang et al. 2019)
RADARSAT-2	2007–Present	24	5.55/C-band	Quad	98.6	(Ozkan et al. 2012; Zou et al. 2016; Carvalho et al. 2018; Song et al. 2017; Singha, Vespe, and Trieschmann 2013)
TerraSAR-X	2007–Present	11	3.11/X-band	Quad	97.2	(Nunziata et al. 2019; Singha et al. 2016; Kim and Jung 2018)
Cosmo-Skymed	2007–Present	1–8	3.1/X-band	Dual	97.86	(Nunziata, Buono, and Migliaccio 2018; Lupidi et al. 2017; Vespe et al. 2011)
RISAT-1	2012–Present	25	5.3/C-band	Quad	97.55	(Dutta et al. 2018; Chaudhary and Kumar 2020; Vanjare et al. 2019)
Sentinel-1A Sentinel-1B	2014–Present 2016–Present	6	3.1/C-band	Dual	98.18	(Arslan 2018; Bayramov, Kada, and Buchroithner 2018; Chaturvedi, Banerjee, and Lele 2020; Cantorna et al. 2019)



362

363 **Figure 9.** Distribution of employed sensor types in oil spill detection studies. The numbers on the graph indicate the frequency  
 364 of sensors' usage in the reviewed literature.



365

366 **Figure 10.** The usage of spaceborne and airborne SAR imagery; and X-, C-, and L-band in oil spill detection studies.  
 367 (combinations of X-, C-, and L- bands) for oil spill detection. The relative detection capacities of SAR are strongly  
 368 connected with the frequency of used instruments, depending on the different penetration capabilities. Because  
 369 SARs of different microwave frequency bands (L-, C-, X-band) interact with different components of the ocean wave  
 370 spectrum, an approach involving multi-frequency characteristics of SAR can offer further information about the  
 371 damping behavior of oil spills (Latini, Fabio, and Jones 2016). For operational purposes, concurrent acquisition (or  
 372 near temporal overlap) of SAR images at L-, C-, and X-band over the same regions may require better examination.  
 373 Considering the potentials of SAR systems acquiring data over the same spill and at the same time, the studies  
 374 adopted a combination of SAR bands less often. As seen in Figure 11, studies combining C- and L-bands are the most  
 375 common (18 studies). There are 11 studies in the reviewed literature that combined all three mentioned bands. In  
 376 addition, 10 papers utilized the combination of X- and C-bands SAR data and just one study established a method  
 377 for the oil spill detection task based on X- and L-band SAR jointly.

378 **4.4. Number of SAR images used in different studies**

379 The statistical results shown in Figure 12 demonstrate the number of spaceborne or airborne images used in a  
 380 specific period per paper. As shown in Figure 12,

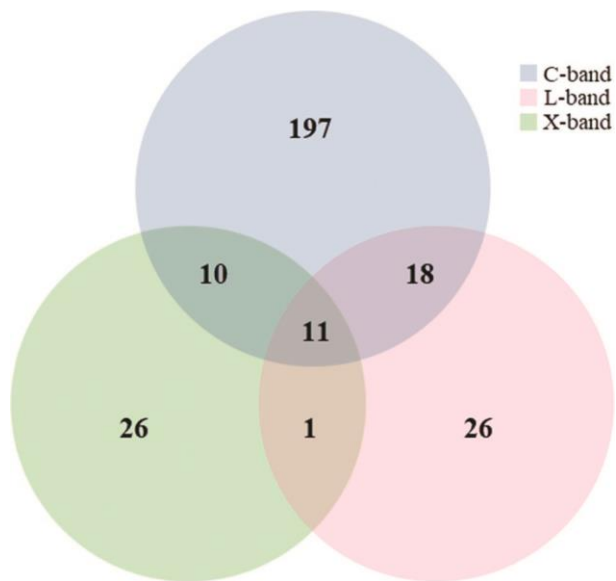


**Figure 11.** Combination of L-, C-, and X-band radar backscatter data used in the reviewed literature on oil spill detection.

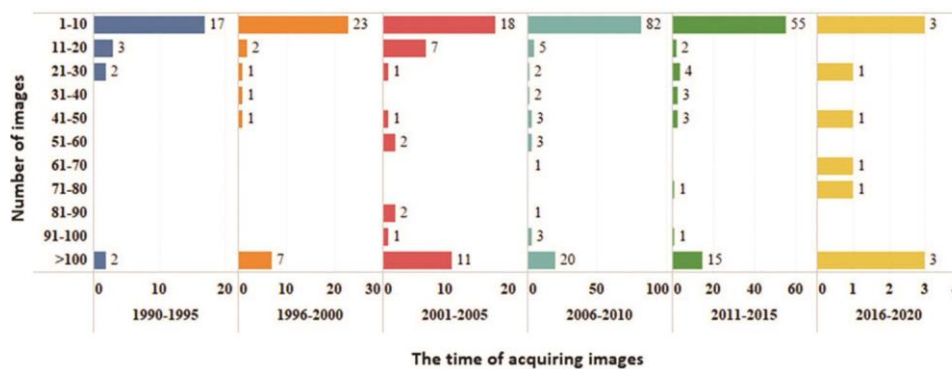


**Figure 12.** Distribution of the number of spaceborne and airborne images per time period.

381 most of the reviewed studies employed the images acquired during 2006–2010, mostly related to the Deepwater  
 382 Horizon oil spill in the Gulf of Mexico, as indicated in Figure 7.

383 **4.5. SAR polarization modes used in oil spill detection**

384 The availability of advanced polarimetric SAR sensors and the generation of various polarization options allow users  
 385 to select the most suitable SAR observations for oil spill detection in various ocean conditions. Polarization options  
 386 could be single-pol, dual-pol, quad-pol, and hybrid/compact-pol. The single-pol SAR provides one channel of SAR  
 387 data in either HH, HV, VH, or VV. Different polarizations make it possible to observe different features. For example,  
 388 from an oil spill detection viewpoint, an oil spill incident can easily be observed in the VV SAR polarization, while  
 389 other corresponding polarizations may not observe it in such an obvious way. SAR images obtained in single-pol HH  
 390 or VV are widely used in operational services (Ivonin et al. 2020).

391 A linear dual-pol SAR system transmits one polarization and receives two, resulting in either HH/HV or VH/VV  
 392 imagery. A dual-pol SAR system provides additional information about surface features through the different and  
 393 complementary echoes compared to a single-pol system. A quad-pol system would alternate between transmitting  
 394 H and V radar signals and coherently receive both H and V, resulting in HH, HV, VH, and VV imagery. Finally, a hybrid-

395 pol transmits a circularly polarized radar signal (right or left) and coherently receives H and V, also known as  
 396 compact-pol.

397 The backscattered signal level from the ocean surface is higher for single-pol VV than for HH-pol (Valenzuela  
 398 1978). Therefore, the VV channel is often preferred to HH for oil spill monitoring (Angelliaume et al. 2018). As  
 399 presented in Figure 13, 133 papers have used single-pol SAR data from all the screened studies. In these studies, 44  
 400 and 89 papers have used HH and VV polarization, respectively. This result is expectable since VV polarization is  
 401 favorable for marine SAR applications.

402 In addition, a total of 40 papers utilized dual-pol SAR imagery, of which HH-VV, HH-HV, and VV-VH were used 32,  
 403 3, and 5 times, respectively. Moreover, a total of 81 and 29 papers used full and hybrid polarization, respectively.  
 404 Since most of the available spaceborne SAR sensors have a moderate noise floor (refer to Table 5), the cross-  
 405 polarization (HV or VH) channels have the most negligible share in the detection of oil slicks (Angelliaume et al.  
 406 2018).

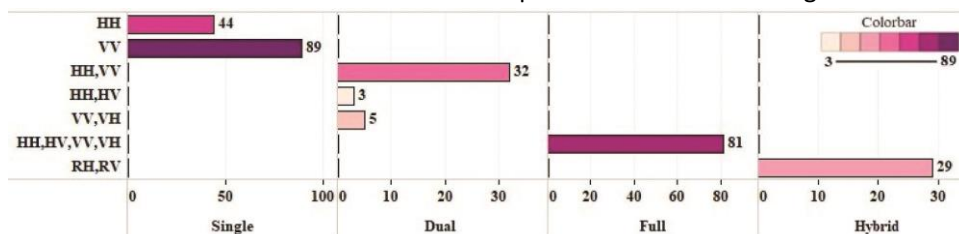
#### 407 4.6. SAR polarization modes and their detection accuracy

408 To evaluate and compare the effects of different types of SAR polarizations on the overall accuracy (OA) of oil spill  
 409 detection schemes, the OA's boxplots were calculated and presented in Figure 14. Herein, the median OA for all  
 410 types of polarization is more than 87%. The median OA of full-pol data is nearly 94%, and the lower and upper  
 411 whiskers extend from 83% to 99%. The more utilization of single-pol data has made the results less consistent, and  
 412 their accuracies depend on the applied methods and marine conditions. The median OA of single-pol data is around  
 413 91%, and the lower and upper whiskers extend from 70% to 99%. Furthermore, the median accuracies of dual-pol  
 414 and hybrid data are 87.6% and 93%, respectively. According to Figure 14 and the reviewed literature (e.g.,  
 415 (Ferdinando Nunziata, Gambardella, and Migliaccio 2008; Velotto et al. 2011; Shirvany, Chabert, and Tournet  
 416 2012; Nunziata, Gambardella, and Migliaccio 2013; Skrunes, Brekke, and Eltoft 2014; Salberg, Rudjord, and Schistad  
 417 Solberg 2014)), quad-pol data can improve the detection capability of slicks compared to dual-pol data. It should  
 418 be kept in mind that operational costs will be considerably high when using multi-channel SAR systems.

#### 419 4.7. The effects of NESZ and incidence angle

420 We know from the theories mentioned above that the NESZ and incidence angle are inversely related. According to  
 421 (Skrunes et al. 2018), for incidence angles above 30°, the VV channel provides higher backscattering values, followed  
 422 by the HH channel. The HV channel provides the lowest backscattering. In (Espeseth et al. 2019), the authors found  
 423 that a signal- to-noise ratio (SNR) of at least 10 dB is required to ensure that the scattering properties are not  
 424 affected by noise. Hence, investigating the marine surface's signal level relative to the noise floor is crucial for oil  
 425 spill monitoring (Tong et al. 2019).

426 As mentioned in the current meta-analysis, the UAVSAR system is widely studied for oil spill detection due to its  
 427 very low NESZ (-53 dB). The available satellite-based SAR sensors have higher noise floors (Skrunes, Brekke, and  
 428 Eltoft 2014; Brent Minchew, Jones, and Holt 2012). The acquisition mode, incidence angle, and NESZ values of typical  
 429 spaceborne SAR sensors are listed in Table 5 for a more comprehensive understanding and better comparison.



430  
 431 **Figure 13.** The number of oil spill monitoring studies that used each type of SAR  
 432 polarization.

433 **Table 5.** The acquisition mode, incidence angle, and NESZ values of satellite-borne SAR  
 434 sensors.

Satellite mission	Acquisition Mode	NESZ (dB)	Incidence Angle (deg)	Number of reviewed studies with imaging mode
ERS-1,2	Stripmap	-21 to -24	20-26	14
JERS-1	Stripmap	<-20.5	35	-
SIR-C/X-SAR	fine quad	-22 to -35	15-55	3
RADARSAT-1	Fine	-21	37-47	2
	Standard	-21	20-49	7
	Wide	-21	20-45	12
	ScanSAR narrow	-21		13
	ScanSAR wide	-21	20-49	9
	Extended High	-21	20-49	-
	Extended Low	-21	52-58	1
	ENVISAT ASAR	Image	-20 to -22	15-45
	Alternating polarization, wave, Wide swath, Global monitoring	-19 to -22 -20 to -22 -21 to -26 -32 to -35	15-45 15-45 17-42 17-42	1 - 44 -
ALOS PALSAR	Fine 1	<-23	8-60	3
	Fine 2	<-25	8-60	2
	Polarimetry	<-29	8-30	1
	ScanSAR	<-25	18-43	3
RADARSAT-2	Fine	-28	20-52	1
	Standard	-31	20-45	3
	Wide	-23	20-46	14
	ScanSAR narrow	-23	20-49	5
	ScanSAR wide	-23	49-60	-
	Extended High	-27.5 to -43	18-49	39
	Fine Quad- polarization			
TerraSAR-X	Spotlight (LR)	-23	20-55	-
	Spotlight (HR)	-23	20-55	-
	Stripmap	-22	20-45	15
	ScanSAR	-21	20-45	14
Cosmo Skymed	ScanSAR wide region	-21	18.4-59.9	2
	ScanSAR huge region	-21	18.4-59.9	4
RISAT-1	CRS ScanSAR	-18	12-34	-
	MR ScanSAR	-18	12-55	1
	FR Stripmap1	-18	12-55	3
	FR Stripmap2	-18	12-55	-
Sentinel-1	Stripmap	-22.2	18.3-46.8	-
	Interferometric wide swath	-23.7	29.1-46	8
	Extra wide swath	-23.1	18.9-47	1
	Wave	-26.3	21.6-38	-

435  
 436 Besides, the number of reviewed studies utilized each type of imaging mode is provided.

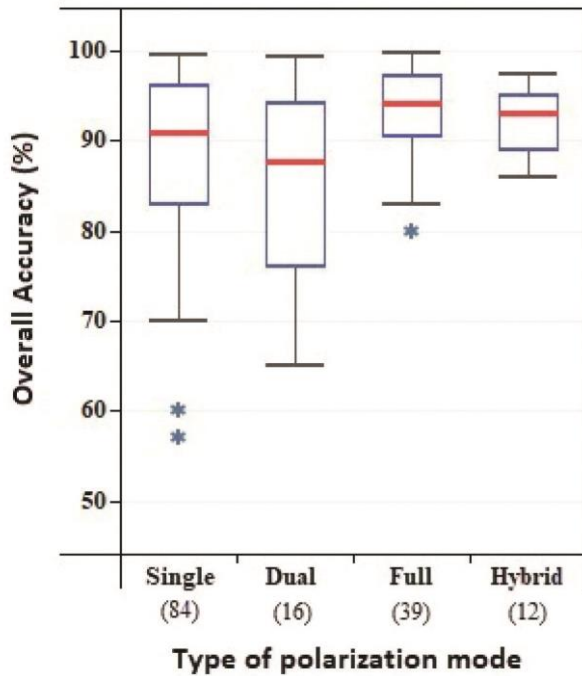
437 **4.8. The effect of wind speed**

438 As investigated in the reviewed literature, the most favorable wind speed range for monitoring oil slicks

439 in SAR images is approximately between 4 m/s and 10 m/s (Espedal et al. 1998; Espedal 1999; Wismann et al. 1998).  
 440 It is also clear from Table 6 that most of the oil spill studies have been done under favorable wind and sea-state  
 441 conditions. The wind speed conditions listed in Table 6 are reported in reviewed papers, based on Quick  
 442 Scatterometer (QuikSCAT)-

**Table 6.** Oil Slick response according to wind speed obtained from reviewed studies.

Wind Speed (m/s)	Oil slick signature	Number of reviewed studies
0–2	Oil slick detection is impracticable. The term “glassy sea” is used for such condition.	36
2–4	No impact of the wind on oil slicks. The detection of hydrocarbons is not easy given the increased lookalikes.	79
4–7	Relatively desirable condition. The wind speed does not have any significant effects on oil slicks. Plus, there are much fewer lookalikes.	115
7–10	Oil slicks begin to be affected by the chop, and Oil-polluted areas gradually disappear from the sea surface water as they are “washed down” by breaking waves.	71
10–12	Due to the dispersion of thin spills, only the thickest oil spills are detectable.	27
>12	Oil slicks are broken up and dispersed, making it difficult and almost impossible to detect, even the thick ones.	12



443  
 444 **Figure 14.** Box-and-whisker plots displaying the effect of different SAR polarizations on the OA.

445 SeaWinds observations (Mercier and Girard-Arduin 2005; Quintero-Marmol et al. 2003; Migliaccio et al. 2007; Shao  
 446 et al. 2008; Mercier and Arduin 2006b), underwater gliders for in-situ ocean measurements, and Cross Calibrated  
 447 Multi-Platform (CCMP) wind data (Tian, Huang, and Hongga 2017). Moreover, in some of the papers, these  
 448 conditions were estimated and retrieved from SAR images using the CMOD4/5 model (CMOD is a C-band geophysical  
 449 model that provides an empirical relation between the radar backscatter sensed from the roughened sea surface

450 and wind speed) (Najoui et al. 2018; Vijayakumar and Rukmini 2016; Mera et al. 2017; Hersbach, Stoffelen, and de  
451 Haan 2007; Garcia-Pineda et al. 2013; Kim et al. 2015).

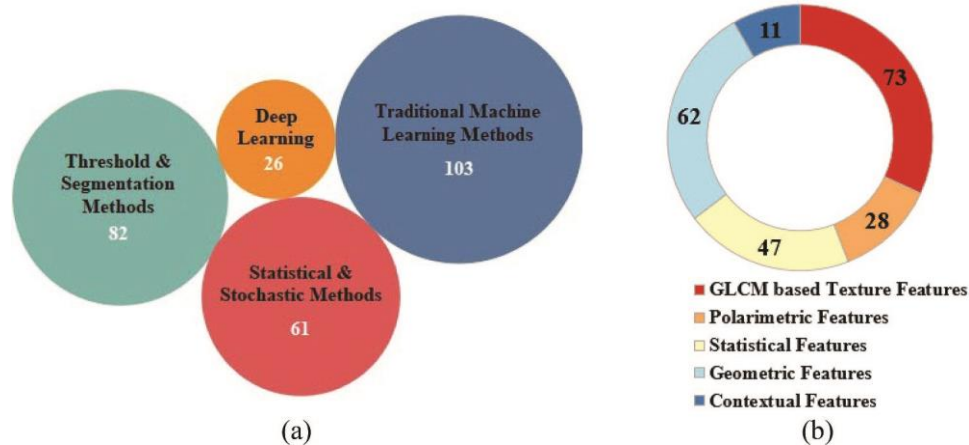
#### 452 4.9. Different analytical oil spill detection methods

453 The detection of oil spills in SAR data generally comprises segmentation, feature extraction, and classification  
454 procedures (Brekke and Solberg 2005a; A. H. S. Solberg, Brekke, and Husoy 2007). Different algorithms have been  
455 presented in the literature for the detection of oil spills. In the current meta-analysis, we summarized the common  
456 and widely used oil detection methods into four categories: traditional machine learning approaches, deep learning  
457 (DL) methods, threshold and segmentation techniques, and statistical algorithms.

458 The main common traditional and machine learning methods employed for detection of oil spills are as follows:  
459 support vector machine (SVM) (Hassani, Sahebi, and Asiyabi 2020; Cao, Linlin, and Clausi 2017; Xu, Jonathan, and  
460 Brenning 2014; Zhang et al. 2017; Mera et al. 2017; Zou et al. 2016), Decision Tree (Topouzelis and Psyllos 2012;  
461 Mihoub and Hassini 2014; Konik and Bradtke 2016; Akar, Süzen, and Kaymakci 2011), Maximum likelihood (Zhang  
462 et al. 2017; Misra and Balaji 2017), Naïve Bayes (Chehresa et al. 2016), Mahalanobis distance (Yang, Ying, and Zhu  
463 2017), Random forest (RF) (Tong et al. 2019), k-means (Skrunes, Brekke, and Eltoft 2014), Classification And  
464 Regression Trees (CART) (Mera et al. 2014) and Artificial Neural Networks (ANNs). Moreover, the most conventional  
465 deep Learning (DL) methods in oil spill detection scheme include convolutional neural network (CNNs) (Guo, Wei,  
466 and Jubai 2018; Temitope Yekeen, Balogun, and Wan Yusof 2020; Cantorna et al. 2019; Zeng and Wang 2020),  
467 Generative Adversarial Networks (GANs) (Yu et al. 2018), deep belief networks (DBNs) (Chen et al. 2017), and  
468 Autoencoders (AEs) (Chen et al. 2017). Widely used statistical approaches include statistical region-based classifier  
469 (Genovez et al. 2019), Markov chain (Yao et al. 2014; Mercier et al. 2003), region- based generalized likelihood ratio  
470 test (GLRT) (Chang et al. 2008; Chang, Cheng, and Tang 2005), logistic regression (Cantorna et al. 2019). Threshold  
471 and segmentation methods mainly consist of adaptive and hysteresis thresholding, edge detection, and entropy  
472 approaches such as the maximum descriptive length algorithm (Montali et al. 2006; Galland, Refregier, and Germain  
473 2004; Pelizzari and Bioucas-Dias 2007; Yu et al. 2017; Li, Jia, and Velotto 2016b).

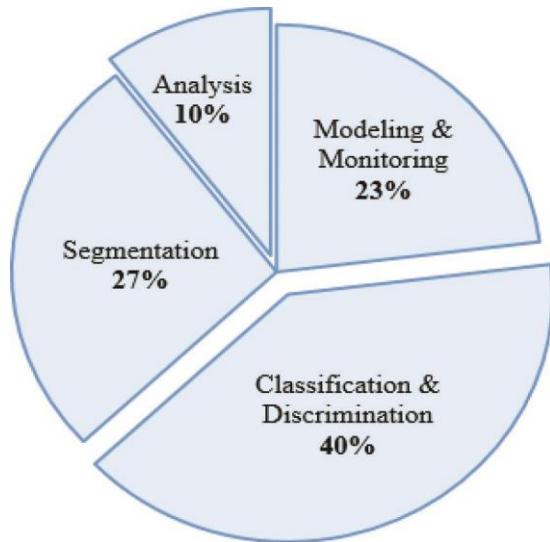
474 As displayed in Figure 15(a), about 103 studies adopted traditional machine learning approaches in the reviewed  
475 literature. In addition, the number of segmentation techniques, statistical methods, and DL algorithms were 82, 61,  
476 and 26, respectively.

477 Moreover, feature (parameters of the dark formations) extraction is a critical step in the oil spill detection  
478 schemes, making it possible to use a group of features to distinguish oil slicks and lookalikes. Figure 15(b) presents  
479 the more common features



480 **Figure 15.** (a) The number of studies associated with each oil detection strategy. (b) The number of publications associated with  
481 different types of features extracted from SAR data.

481 adopted in oil spill detection studies. These features can be separated into five major groups: (1) features referring  
482 to the geometrical properties of dark formations (e.g., area, perimeter, shape) (Karathanassi et al. 2006; Brekke and  
483 Solberg 2005b), (2) features concerning the physical/statistical behavior of oil spills (e.g., mean, max, standard  
484 deviation, and ratios of backscattering coefficient values) (Karathanassi et al. 2006; Topouzelis 2008), (3) features  
485 denoting to the oil spill context (e.g., presence of rig/ship, distance to ship) (Brekke and Solberg 2005b; Topouzelis,  
486 Stathakis, and Karathanassi 2009; Chehresa et al. 2016), (4) derivatives of gray-level co-occurrence matrix known as  
487 GLCM-based texture features (e.g.,



488 contrast, correlation, entropy, energy) (Chehresa et al. 2016; Yang, Ying, and Zhu 2017; Guo, Danni, and Jubai 2017),  
489 and (5) features extracted from different polarimetric SAR images (e.g., degree of polarization, alpha angle) (Song  
490 et al. 2017; Zhang et al. 2017; Li et al. 2018).

#### 492 **4.10. Strategies in oil spill detection studies**

493 As discussed earlier, the reviewed papers used different methods to deal with oil spill detection issues. In general,  
494 these methods follow related sub-objectives in line with the primary objective (i.e., oil spill detection). Figure 16  
495 illustrates the

496 **Figure 16.** Different strategies in oil spill  
497 detection.

498 different types of sub-objectives considered in the  
499 reviewed studies. As shown, 40% of studies were  
500 benefited from “classification and discrimination”  
501 strategies followed by “modelling and monitoring,”  
502 which accounts for 23% of the studies. The “modelling  
503 and monitoring” group includes various strategies,  
504 including monitoring the spatial distribution and  
505 primary sources of oil spills, visual interpretation,  
506 contamination probability modeling and assessment,  
507 time series analysis and oil spill frequency modeling,  
508 numerical simulations to simulate the trajectories of the  
509 oil spills, oil slick trajectory forecasting model, and  
510 characterizing oil- water mixing.

511 Based on Figure 16, 27% of the studies adopted their  
512 strategies based on image segmentation. Furthermore,  
513 only 10% of studies are categorized as “analysis” group,  
514 mainly focused on interpreting

515 SAR backscattering mechanisms over oil-covered waters, oil-polluted areas’ backscattering simulation,  
516 characterizing the scattering from oil spills and biogenic surface films under different wind conditions, and  
517 assessment of experience from a field experiment. Studies associate with multi- sensor, multi-polarization and  
518 multi-frequency analyses of different SAR systems in oil spill events and their response in oil-polluted areas are also  
519 involved in this group.

## 520 **5. Conclusions and future research needs**

521 In this paper, we presented a comprehensive review and meta-analysis of oil spill detection studies. Our research  
522 provides a systematic investigation of indexed research studies’ compilation and analysis, focusing on several  
523 features, such as data, platform, and sensor type, SAR imaging mode, microwave carrier frequency (e.g., L-, C-, and  
524 X-bands), polarization option (i.e., single-pol, dual-pol, full-pol, and compact- pol), incidence angle, and wind speed  
525 condition. Furthermore, it gives a comprehensive overview of the approaches established to deal with the oil spill  
526 detection task through SAR imagery. The current meta-analysis is the only research conducted to provide both  
527 descriptive and quantitative investigation of oil spill studies using a database containing 308 eligible papers, of which  
528 230 are journal papers and 78 are conference papers. A summarization of the paper’s content and crucial findings  
529 are given in the following:

- 530 • The summarized papers in the present meta- analysis have been published in 89 different journals and two  
531 conferences. From all of these publications, about 42% of them were published from 2016 to 2020.
- 532 • Researchers affiliated with institutions in China and Italy account for the bulk of oil spill studies with nearly 20%  
533 and 15% of the database, respectively. Consequently, a significant part of this review study is conducted in  
534 either of these two countries, followed by Norway (8%), USA (7%).
- 535 • Since the coverage of the spaceborne missions is much more extensive than that of the airborne missions, most  
536 of the reviewed studies employed spaceborne data sets in maritime oil spill detection with a 93% share.
- 537 • In terms of sensor type, ENVISAT (84 studies),  
538 RADARSAT-2 (82 studies), ERS-2 (69 studies), ERS-1 (52 studies), RADARSAT-1 (45 studies), and TerraSAR-X (40  
539 studies) are the most frequently studied data sources.
- 540 • Most of the reviewed studies employed the images acquired during 2006–2010, which could be related to the  
541 Deepwater Horizon oil spill in the Gulf of Mexico.
- 542 • From the polarization perspective, single-pol (133 studies) and full-pol (81 studies) SAR data have a significant  
543 share in the reviewed literature with a median overall accuracy of 94% and 91%, respectively. Furthermore,  
544 the median accuracy of dual-pol (40 studies) and Hybrid (29 studies) data are 87.6% and 93%, respectively.
- 545 • Reviewed studies indicated that C-band radar had been used widely in the oil spill detection task with 236  
546 studies, followed by L-band (56 studies) and X-band (48 studies).
- 547 • From a methodology point of view, about 103 studies adopted different traditional classification methods in  
548 the reviewed literature. Additionally, the number of studies that utilized segmentation methods, statistical  
549 methods, and DL algorithms were 82, 61, and 26, respectively.
- 550 • Environmental wind speed condition measurements play a significant role in oil spill detection. About 68% of  
551 reviewed papers adopted these measurements.

552 SAR sensors are efficient RS tools for oil spill detection, and various techniques have been proposed to cope with  
553 the monitoring of oil pollution using SAR data in recent decades. Nevertheless, there is a need to develop real-time  
554 monitoring systems. Providing techniques based on cloud computing services and proposed automatic DL models,

555 considering the continuous development in computer vision will significantly increase the success in this area. In  
556 addition, it is still necessary to extensively explore the potential of compact hybrid polarization, which is currently  
557 provided operationally by the RADARSAT Constellation Mission, for oil spill monitoring. It is also expected from the  
558 scientific community, i.e., from RS experts to environmental monitoring specialists, to access various multi-sensor  
559 images collected over different locations and open-source annotated datasets related to oil spill events. This will  
560 increase the speed of achieving new detection algorithms that are desperately needed to protect the marine  
561 environment. A detailed investigation and review of oil spill detection methods in the literature is also absent.

## 562 ORCID

563 Hamid Jafarzadeh  <http://orcid.org/0000-0001-7785-1872>  
564 Masoud Mahdianpari  <http://orcid.org/0000-0002-7234-959X>  
565 Fariba Mohammadimanesh  [http://orcid.org/0000-0002-](http://orcid.org/0000-0002-9472-2324)  
566 9472-2324

## 567 References

- 568 Akar, S., M. L. Süzen, and N. Kaymakci. 2011. "Detection and Object-Based Classification of Offshore Oil Slicks Using ENVISAT-ASAR  
569 Images." *Environmental Monitoring and Assessment* 183 (1): 409–423. doi:10.1007/s10661-011-1929-6.
- 570 Akkartal, A., and F. Sunar. 2008. "The Usage of RADAR Images in Oil Spill Detection." *The International Archives of the Photogrammetry,  
571 Remote Sensing and Spatial Information Sciences* 37: 271–277.
- 572 Alpers, W., B. Holt, and K. Zeng. 2017. "Oil Spill Detection by Imaging Radars: Challenges and Pitfalls." *Remote Sensing of Environment*  
573 201 (November): 133–147. doi:10.1016/j.rse.2017.09.002.
- 574 Alpers, W., P. Brandt, A. Lazar, D. Dagherne, B. Sow, S. Faye, M. Hansen, A. Rubino, P.-M. Poulain, and P. Bremer. 2013. "A Small-Scale  
575 Oceanic Eddy off the Coast of West Africa Studied by Multi-Sensor Satellite and Surface Drifter Data." *Remote Sensing of Environment*  
576 129: 132–143. doi:10.1016/j.rse.2012.10.032.
- 577 Angelliaume, S., P. C. Dubois-Fernandez, C. E. Jones, B. Holt, B. Minchew, E. Amri, and V. Mieggebielle. 2018. "SAR Imagery for Detecting  
578 Sea Surface Slicks: Performance Assessment of Polarization-Dependent Parameters." *IEEE Transactions on Geoscience and Remote  
579 Sensing* 56 (8): 4237–4257. doi:10.1109/TGRS.2018.2803216.
- 580 Araújo, R. T. S., F. N. S. de Medeiros, R. C. S. Costa, R. C. P. Marques, R. B. Moreira, and J. L. Silva. 2004. "Locating Oil Spill in SAR Images  
581 Using Wavelets and Region Growing." In *Innovations in Applied Artificial Intelligence*, edited by B. Orchard, C. Yang, and M. Ali, 1184–  
582 1193. Lecture Notes in Computer Science. Berlin, Heidelberg: Springer. doi:10.1007/978-3-540-24677-0\_121.
- 583 Arduin, F. G., G. Mercier, and R. Garello. 2003. "Oil Slick Detection by SAR Imagery: Potential and Limitation."
- 584 Arslan, N. 2018. "Assessment of Oil Spills Using Sentinel 1 C-Band SAR and Landsat 8 Multispectral Sensors." *Environmental Monitoring  
585 and Assessment* 190 (11): 637.  
586 doi:10.1007/s10661-018-7017-4.
- 587 Asl, D., D. S. Samira, M. B. Dukhovskoy, and I. R. MacDonald. 2017. "Hindcast Modeling of Oil Slick Persistence from Natural  
588 Seeps." *Remote Sensing of Environment*  
589 189 (February): 96–107. doi:10.1016/j.rse.2016.11.003.
- 590 Bandiera, F., A. Masciullo, and G. Ricci. 2014. "A Bayesian Approach to Oil Slicks Edge Detection Based on SAR Data." *IEEE Transactions  
591 on Geoscience and Remote Sensing* 52 (5): 2901–2909. doi:10.1109/TGRS.2013.2267594.
- 592 Barni, M., M. Betti, and A. Mecocci. 1995. "A Fuzzy Approach to Oil Spill Detection an SAR Images." In *1995 International Geoscience  
593 and Remote Sensing Symposium, IGARSS '95, Firenze, Italy. Quantitative Remote Sensing for Science and Applications*, 1:157–159.  
594 doi:10.1109/IGARSS.1995.519676.
- 595 Bayındır, C. J., D. Frost, and C. F. Barnes. 2018. "Assessment and Enhancement of SAR Noncoherent Change Detection of Sea-Surface  
596 Oil Spills." *IEEE Journal of Oceanic Engineering* 43 (1): 211–220. doi:10.1109/JOE.2017.2714818.
- 597 Bayramov, E., M. Kada, and M. Buchroithner. 2018. "Monitoring Oil Spill Hotspots, Contamination Probability Modelling and Assessment  
598 of Coastal Impacts in the Caspian Sea Using SENTINEL-1, LANDSAT-8, RADARSAT, ENVISAT and ERS Satellite Sensors." *Journal of  
599 Operational Oceanography* 11 (1): 27–43. Institute of Marine Engineering, Science and Technology.  
600 doi:10.1080/1755876X.2018.1438343.
- 601 Brekke, C., and A. H. S. Solberg. 2005a. "Feature Extraction for Oil Spill Detection Based on SAR Images." In *Image Analysis*, edited by  
602 H. Kalviainen, J. Parkkinen, and A. Kaarna, 75–84. Lecture Notes in Computer Science. Berlin, Heidelberg: Springer.  
603 doi:10.1007/11499145\_9.  
604

605 Brekke, C., and A. H. S. Solberg. 2005b. "Oil Spill Detection by Satellite Remote Sensing." *Remote Sensing of Environment* 95 (1): 1–13.  
606 doi:10.1016/j.rse.2004.11.015.

607 Buono, A., F. Nunziata, C. R. de Macedo, D. Velotto, and M. Migliaccio. 2019. "A Sensitivity Analysis of the Standard Deviation of the  
608 Copolarized Phase Difference for Sea Oil  
609 Slick Observation." *IEEE Transactions on Geoscience and Remote Sensing* 57 (4): 2022–2030. doi:10.1109/ TGRS.2018.2870738.

610 Cantorna, D., C. Dafonte, A. Iglesias, and B. Arcay. 2019. "Oil Spill Segmentation in SAR Images Using Convolutional Neural Networks. A  
611 Comparative Analysis with Clustering and Logistic Regression Algorithms." *Applied Soft Computing* 84 (November): 105716.  
612 doi:10.1016/j. asoc.2019.105716.

613 Cao, Y., X. Linlin, and D. Clausi. 2017. "Exploring the Potential of Active Learning for Automatic Identification of Marine Oil  
614 Spills Using 10-Year (2004–2013) RADARSAT Data." *Remote  
615 Sensing* 9 (10): 1041. doi:10.3390/rs9101041.  
616 Multidisciplinary Digital Publishing Institute.

617 Caruso, M. J., M. Migliaccio, J. T. Hargrove, O. Garcia-Pineda, and H. C. Graber. 2013. "Oil Spills and Slicks Imaged by Synthetic Aperture  
618 Radar." *Oceanography* 26 (2): 112–123. JSTOR. doi:10.5670/oceanog.2013.34.

619 Carvalho, G., P. J. de Araújo, E. Minnett, T. Paes, F. P. De Miranda, and L. Landau. 2018. "Refined Analysis of RADARSAT-2 Measurements  
620 to Discriminate Two Petrogenic Oil-Slick Categories: Seeps versus Spills." *Journal of Marine Science and Engineering* 6 (4): 153.  
621 doi:10.3390/jmse6040153. Multidisciplinary Digital Publishing Institute.

622 Carvalho, G. D. A., P. J. Minnett, E. T. Paes, F. P. De Miranda, and L. Landau. 2019. "Oil-Slick Category Discrimination (Seeps Vs. Spills):  
623 A Linear Discriminant Analysis Using RADARSAT-2 Backscatter Coefficients ( $\Sigma$ ,  $B^\circ$ , and  $\Gamma$ ) in Campeche Bay (Gulf of Mexico)." *Remote  
624 Sensing* 11 (14): 1652. doi:10.3390/rs11141652. Multidisciplinary Digital  
625 Publishing Institute.

626 Carvalho, G. D. A., P. J. Minnett, N. F. F. Ebecken, and L. Landau. 2020. "Classification of Oil Slicks and Look-Alike Slicks: A Linear  
627 Discriminant Analysis of Microwave, Infrared, and Optical Satellite Measurements." *Remote Sensing* 12 (13): 2078.  
628 doi:10.3390/rs12132078. Multidisciplinary Digital Publishing Institute.

629 Carvalho, G. D. A., P. P. J. Minnett, F. P. De Miranda, L. Landau, and F. Moreira. 2016. "The Use of a RADARSAT-Derived Long-Term  
630 Dataset to Investigate the Sea Surface Expressions of Human-Related Oil Spills and Naturally Occurring Oil Seeps in Campeche Bay,  
631 Gulf of Mexico." *Canadian Journal of Remote Sensing* 42 (May3): 307–321. doi:10.1080/07038992.2016.1173532.

632 Ceyhun, G. Ç. 2014. "The Impact of Shipping Accidents on Marine Environment: A Study of Turkish Seas." *European Scientific Journal*  
633 10. [https://www.semanticscholar.org/paper/THE-IMPACT-OF-SHIPPING-ACCIDENTS-ON-MARINE  
634 - A - S T U D Y - C e y h u n  
635 /3c91b50aabf1ba42fc2cb00faaf1e1f9f20a76db](https://www.semanticscholar.org/paper/THE-IMPACT-OF-SHIPPING-ACCIDENTS-ON-MARINE-A-S-T-U-D-Y-C-e-y-h-u-n/3c91b50aabf1ba42fc2cb00faaf1e1f9f20a76db)

636 Chang, L., C. M. Cheng, and Z. S. Tang. 2005. "An Automatic Detection of Oil Spills in Sar Images by Using Image Segmentation Approach."  
637 In *Proceedings. 2005 IEEE International Geoscience and Remote Sensing Symposium, 2005*. IGARSS '05. Seoul, Korea (South), 2:1021–  
638 1024. doi:10.1109/IGARSS.2005.1525287.

639 Chang, L. Z., S. Tang, S. H. Chang, and Y.-L. Chang. 2008. "A Region-Based GLRT Detection of Oil Spills in SAR Images." *Pattern Recognition  
640 Letters* 29 (14): 1915–1923. doi:10.1016/j. patrec.2008.05.022.

641 Chaturvedi, S. K., S. Banerjee, and S. Lele. 2020. "An Assessment of Oil Spill Detection Using Sentinel 1 SAR-C Images." *Journal of Ocean  
642 Engineering and Science* 5 (2): 116–135. doi:10.1016/j.joes.2019.09.004.

643 Chaudhary, V., and S. Kumar. 2020. "Marine Oil Slicks Detection Using Spaceborne and Airborne SAR Data." *Advances in Space Research*  
644 66 (4): 854–872. doi:10.1016/j. asr.2020.05.003.

645 Chehresa, S., A. Amirkhani, G.-A. Rezairad, and M. R. Mosavi. 2016. "Optimum Features Selection for Oil Spill Detection in SAR Image."  
646 *Journal of the Indian Society of Remote Sensing* 44 (5): 775–787. doi:10.1007/s12524-016-0553-x.

647 Chen, G., L. Yu, G. Sun, and Y. Zhang. 2017. "Application of Deep Networks to Oil Spill Detection Using Polarimetric Synthetic Aperture  
648 Radar Images." *Applied Sciences* 7 (10): 968. doi:10.3390/app7100968. Multidisciplinary Digital Publishing Institute.

649 Chen, J., W. Zhang, Z. Wan, L. Sifan, T. Huang, and Y. Fei. 2019. "Oil Spills from Global Tankers: Status Review and Future Governance."  
650 *Journal of Cleaner Production* 227 (August): 20–32. doi:10.1016/j.jclepro.2019.04.020.

651 Cheng, Y., L. Xiaofeng, X. Qing, O. Garcia-Pineda, O. B. Andersen, and W. G. Pichel. 2011. "SAR Observation and Model Tracking of an  
652 Oil Spill Event in Coastal Waters." *Marine Pollution Bulletin* 62 (2): 350–363. doi:10.1016/j.  
653 marpolbul.2010.10.005.

654 Chierchia, G., D. Cozzolino, G. Poggi, and L. Verdoliva. 2017. "SAR Image Despeckling through Convolutional Neural Networks." In  
655 *2017 IEEE International Geoscience and Remote Sensing Symposium (IGARSS)*, Fort Worth, TX, USA, 5438–5441.  
656 doi:10.1109/IGARSS.2017.8128234.

657 Clemente-Colon, P., and X.-H. Yan. 2000. "Low-Backscatter Ocean Features in Synthetic Aperture Radar Imagery." *Johns Hopkins APL  
658 Technical Digest* 21 (1): 116–121. Johns Hopkins University Applied Physics Laboratory.

659 Congress, U. S. 1991. *Office of Technology Assessment, Bioremediation for Marine Oil Spills-background Paper*. Washington, DC:  
660 Government Printing Office OTA-BP-O-70.

661 Dabboor, M., S. Singha, B. Montpetit, B. Deschamps, and D. Flett. 2018. "Assessment of Simulated Compact Polarimetry of the RCM  
662 Medium Resolution Sar Modes for Oil Spill Detection." In *IGARSS 2018-2018 IEEE International Geoscience and Remote Sensing*  
663 *Symposium*, Valencia, Spain, 2416–2419. doi:10.1109/IGARSS.2018.8517756.

664 Dabboor, M., S. Singha, B. Montpetit, B. Deschamps, and  
665 D. Flett. 2019. "Pre-Launch Assessment of RADARSAT Constellation Mission Medium Resolution Modes for Sea Oil Slicks and Lookalike  
666 Discrimination." *Canadian Journal of Remote Sensing* 45 (July): 530–549. doi:10.1080/07038992.2019.1659722.

667 Dagestad, K.-F., J. Horstmann, A. Mouche, W. Perrie, H. Shen, B. Zhang, L. Xiaofeng et al. 2013. "Wind Retrieval from Synthetic  
668 Aperture Radar- an Overview." *SeaSAR 2012* 709 (March): 25.

669 Danklmayer, A., B. J. Doring, M. Schwerdt, and M. Chandra. 2009. "Assessment of Atmospheric Propagation Effects in SAR Images."  
670 *IEEE Transactions on Geoscience and Remote Sensing* 47 (10): 3507–3518. doi:10.1109/TGRS.2009.2022271. de Oliveira, O. M. C., A.  
671 F. D. S. Queiroz, J. R. Cerqueira,  
672 S. A. R. Soares, K. S. Garcia, A. P. Filho, M. D. L. D. S. Rosa, C. M. Suzart, L. D. L. Pinheiro, and Í. T. A. Moreira. 2020. "Environmental  
673 Disaster in the Northeast Coast of Brazil: Forensic Geochemistry in the Identification of the Source of the Oily Material." *Marine*  
674 *Pollution Bulletin* 160 (November): 111597. doi:10.1016/j.marpolbul.2020.111597.

675 Dutta, S., M. Joseph, E. V. Suriya Sita Kumari, and A. V. Venkateswara Prasad. 2018. "Automated Approach for Extraction of Oil Spill  
676 from SAR Imagery." *Journal of the Indian Society of Remote Sensing* 46 (4): 633–639.  
677 doi:10.1007/s12524-017-0728-0.

678 El-Magad, A., M. Z. Islam, A. M. Abdulaziz, and E. M. Ali. 2020. "The Potentiality of Operational Mapping of Oil Pollution in the  
679 Mediterranean Sea near the Entrance of the Suez Canal Using Sentinel-1 SAR Data." *Remote Sensing* 12 (8): 1352.  
680 doi:10.3390/rs12081352. Multidisciplinary Digital  
681 Publishing Institute.

682 Espedal, H. A. 1999. "Satellite SAR Oil Spill Detection Using Wind History Information." *International Journal of Remote Sensing* 20  
683 (1): 49–65. doi:10.1080/014311699213596. Taylor & Francis.

684 Espedal, H. A., and O. M. Johannessen. 2000. "Detection of Oil Spills near Offshore Installations Using Synthetic Aperture Radar (SAR)."  
685 *International Journal of Remote Sensing* 21 (July): 2141–2144. doi:10.1080/01431160050029468.

686 Espedal, H. A., O. M. Johannessen, J. A. Johannessen, E. Dano, D. R. Lyzenga, and J. C. Knulst. 1998. "COASTWATCH'95: ERS 1/2 SAR  
687 Detection of Natural Film on the Ocean Surface." *Journal of Geophysical Research* 103 (October): 24.  
688 doi:10.1029/98JC01660.

689 Espeseth, M. M., S. Skrunes, C. Brekke, and M. Johansson. 2019. "The Impact of Additive Noise on Polarimetric Radarsat-2 Data Covering  
690 Oil Slicks." In *IGARSS 2019- 2019 IEEE International Geoscience and Remote Sensing Symposium*, Yokohama, Japan, 5756–5759.  
691 doi:10.1109/IGARSS.2019.8899787.

692 Espeseth, M. M., S. Skrunes, C. E. Jones, C. Brekke, B. Holt, and A. P. Doulgeris. 2017. "Analysis of Evolving Oil Spills in Full-Polarimetric  
693 and Hybrid-Polarity SAR." *IEEE Transactions on Geoscience and Remote Sensing* 55 (7): 4190–4210. doi:10.1109/TGRS.2017.2690001.

694 Fan, J., F. Zhang, D. Zhao, and J. Wang. 2015. "Oil Spill Monitoring Based on SAR Remote Sensing Imagery." *Aquatic Procedia, Maritime*  
695 *Oil Spill Response* 3 (March): 112–118. doi:10.1016/j.aqpro.2015.02.234. Fazeres-Ferradosa, T., P. Rosa-Santos, F. Taveira-Pinto, E.  
696 Vanem, H. Carvalho, and J. Correia. 2019. "Editorial: Advanced Research on Offshore Structures and Foundation Design: Part 1."  
697 *Proceedings of the Institution of Civil Engineers - Maritime Engineering* 172 (4): 118–123. doi:10.1680/jmaen.2019.172.4.118. ICE  
698 Publishing.

699 Fingas, M. 2011. "Chapter 13 - Weather Effects on Oil Spill Countermeasures." In *Oil Spill Science and Technology*, edited by M. Fingas,  
700 339–426. Boston: Gulf Professional Publishing. doi:10.1016/B978-1-85617-943-0.10013-9. Fingas, M., and C. Brown. 2014. "Review of  
701 Oil Spill Remote Sensing." *Marine Pollution Bulletin* 83 (1): 9–23. doi:10.1016/j.marpolbul.2014.03.059.

702 Fingas, M., and C. E. Brown. 2018. "A Review of Oil Spill Remote Sensing." *Sensors* 18 (1): 91. doi:10.3390/s18010091. Multidisciplinary  
703 Digital Publishing Institute.

704 Fingas, M. F., and C. E. Brown. 1997. "Review of Oil Spill Remote Sensing." *Spill Science & Technology Bulletin, the Second International*  
705 *Symposium on Oil Spills* 4 (4): 199–208. doi:10.1016/S1353-2561(98)00023-1.

706 Frulla, L. A., J. A. Milovich, H. Karszenbaum, and D. A. Gagliardini. 1998. "Radiometric Corrections and Calibration of SAR Images." In  
707 *IGARSS '98. Sensing and Managing the Environment. 1998 IEEE International Geoscience and Remote Sensing. Symposium*  
708 *Proceedings. (Cat. No.98CH36174)*, Seattle, WA, USA, 2: 1147–1149. doi:10.1109/IGARSS.1998.699700.

709 Fustes, D., D. Cantorna, C. Dafonte, B. Arcay, A. Iglesias, and M. Manteiga. 2014. "A Cloud-Integrated Web Platform for Marine  
710 Monitoring Using GIS and Remote Sensing. Application to Oil Spill Detection through SAR Images." *Future Generation Computer*  
711 *Systems, Special Section: Distributed Solutions for Ubiquitous Computing and Ambient Intelligence* 34 (May): 155–160. doi:10.1016/j.  
712 future.2013.09.020.

713 Gade, M., W. Alpers, H. Hühnerfuss, H. Masuko, and T. Kobayashi. 1998. "Imaging of Biogenic and Anthropogenic Ocean Surface Films  
714 by the  
715 Multifrequency/Multipolarization SIR-C/X-SAR." *Journal of Geophysical Research: Oceans* 103 (C9): 18851–18866.  
716 doi:10.1029/97JC01915.

717 Galland, F., P. Refregier, and O. Germain. 2004. "Synthetic Aperture Radar Oil Spill Segmentation by Stochastic Complexity  
718 Minimization." *IEEE Geoscience and Remote Sensing Letters* 1 (October): 295–299. doi:10.1109/LGRS.2004.835346.

719 Garcia-Pineda, O., G. Staples, C. E. Jones, C. Hu, B. Holt, V. Kourafalou, G. Graettinger, L. DiPinto, E. Ramirez, D. Streett, J. Cho, G.  
720 A. Swayze, S. Sun, D. Garcia, and F. Haces-Garcia. 2020. "Classification of Oil Spill by Thicknesses Using Multiple Remote Sensors."  
721 *Remote Sensing of Environment* 236 (January): 111421. doi:10.1016/j.rse.2019.111421.

722 Garcia-Pineda, O., I. R. MacDonald, X. Li, C. R. Jackson, and W. G. Pichel. 2013. "Oil Spill Mapping and Measurement in the Gulf of Mexico  
723 with Textural Classifier Neural Network Algorithm (TCNNA)." *IEEE Journal of Selected Topics in Applied Earth Observations and  
724 Remote Sensing* 6 (6): 2517–2525. doi:10.1109/JSTARS.2013.2244061.

725 Garcia-Pineda, O., J. Holmes, M. Rissing, R. Jones, C. Wobus, J. Svejksky, and M. Hess. 2017. "Detection of Oil near Shorelines during  
726 the Deepwater Horizon Oil Spill Using Synthetic Aperture Radar (SAR)." *Remote Sensing* 9 (6): 567. doi:10.3390/rs9060567.  
727 Multidisciplinary Digital Publishing Institute.

728 Genovez, P. C., C. E. Jones, S. J. S. Sant'Anna, and C. C. Freitas. 2019. "Oil Slick Characterization Using a Statistical Region-Based Classifier  
729 Applied to UAVSAR Data." *Journal of Marine Science and Engineering* 7 (2): 36. doi:10.3390/jmse7020036. Multidisciplinary Digital  
730 Publishing Institute.

731 Gens, R. 2008. "Oceanographic Applications of SAR Remote Sensing." *GIScience & Remote Sensing* 45 (3): 275–305. doi:10.2747/1548-  
732 1603.45.3.275. Taylor & Francis.

733 Guo, H., G. Wei, and A. Jubai. 2018. "Dark Spot Detection in SAR Images of Oil Spill Using Segnet." *Applied Sciences* 8 (12): 2670.  
734 doi:10.3390/app8122670. Multidisciplinary Digital Publishing Institute.

735 Guo, H., W. Danni, and A. Jubai. 2017. "Discrimination of Oil Slicks and Lookalikes in Polarimetric SAR Images Using CNN." *Sensors* 17  
736 (8): 1837. doi:10.3390/s17081837.  
737 Multidisciplinary Digital Publishing Institute.

738 Hassani, B., M. R. Sahebi, and R. M. Asiyabi. 2020. "Oil Spill Four-Class Classification Using UAVSAR Polarimetric Data." *Ocean Science  
739 Journal* 55 (3): 433–443. doi:10.1007/s12601-020-0023-9.

740 Hersbach, H., A. Stoffelen, and S. de Haan. 2007. "An Improved C-Band Scatterometer Ocean Geophysical Model Function: CMOD5."  
741 *Journal of Geophysical Research (Oceans)* 112 (March): C03006. doi:10.1029/2006JC003743.

742 Hoffman, A. J., and P. Devereaux Jennings. 2011. "The BP Oil Spill as a Cultural Anomaly? Institutional Context, Conflict, and Change."  
743 *Journal of Management Inquiry* 20 (2): 100–112. doi:10.1177/1056492610394940. SAGE  
744 Publications Inc.

745 Holstein, A., M. Kappas, P. Propastin, and T. Renchin. 2018. "Oil Spill Detection in the Kazakhstan Sector of the Caspian Sea with the  
746 Help of ENVISAT ASAR Data." [https://pubag.nal.  
747 usda.gov/catalog/5909939](https://pubag.nal.usda.gov/catalog/5909939)

748 Hu, C., L. Xiaofeng, W. G. Pichel, and F. E. Muller-Karger. 2009. "Detection of Natural Oil Slicks in the NW Gulf of Mexico Using MODIS  
749 Imagery." *Geophysical Research Letters* 36 (1): 1. doi:10.1029/2008GL036119.

750 ITOFF. 2020. *International Tanker Owners Pollution Federation Limited. Oil Tanker Spill Statistics*. London: United Kingdom.

751 Ivanov, A. Y. 2010. "The Oil Spill from a Shipwreck in Kerch Strait: Radar Monitoring and Numerical Modelling." *International Journal of  
752 Remote Sensing* 31 (September): 4853–4868. doi:10.1080/01431161.2010.485215.

753 Ivonin, D., C. Brekke, S. Skrunes, A. Ivanov, and N. Kozhelupova. 2020. "Mineral Oil Slicks Identification Using Dual Co-Polarized Radarsat-  
754 2 and TerraSAR-X SAR Imagery." *Remote Sensing* 12 (7): 1061. doi:10.3390/rs12071061. Multidisciplinary Digital Publishing Institute.

755 Jafarzadeh, H., and M. Hasanlou. 2019a. "Assessing and Comparing the Performance of Endmember Extraction Methods in Multiple  
756 Change Detection Using  
757 Hyperspectral Data." *ISPRS - International Archives of the Photogrammetry, Remote Sensing and Spatial Information Sciences* 4218  
758 (October): 571–575. doi:10.5194/isprs-archives-XLII-4-W18-571-2019.

759 Jafarzadeh, H., and M. Hasanlou. 2019b. "An Unsupervised Binary and Multiple Change Detection Approach for Hyperspectral Imagery  
760 Based on Spectral Unmixing." *IEEE Journal of Selected Topics in Applied Earth Observations and Remote Sensing* 12 (12): 4888–4906.  
761 doi:10.1109/JSTARS.2019.2939133.

762 Jha, M. N., J. Levy, and Y. Gao. 2008. "Advances in Remote Sensing for Oil Spill Disaster Management: State-of-the-Art Sensors  
763 Technology for Oil Spill Surveillance." *Sensors* 8 (1): 236–255. doi:10.3390/s8010236. Molecular Diversity Preservation International.

764 Karathanassi, V., K. Topouzelis, P. Pavlakis, and D. Rokos. 2006. "An Object-oriented Methodology to Detect Oil Spills." *International  
765 Journal of Remote Sensing* 27 (23): 5235–5251.  
766 doi:10.1080/01431160600693575. Taylor & Francis.

767 Keramitsoglou, I., C. Cartalis, and C. T. Kiranoudis. 2006. "Automatic Identification of Oil Spills on Satellite Images." *Environmental  
768 Modelling & Software* 21 (5): 640–652. doi:10.1016/j.envsoft.2004.11.010.

769 Kim, D., and H.-S. Jung. 2018. "Mapping Oil Spills from Dual-Polarized SAR Images Using an Artificial Neural Network: Application to Oil  
770 Spill in the Kerch Strait in November 2007." *Sensors* 18 (7): 2237. doi:10.3390/s18072237. Multidisciplinary Digital Publishing  
771 Institute.

772 Kim, D.-J., W. M. Moon, and Y.-S. Kim. 2010. "Application of TerraSAR-X Data for Emergent Oil-Spill Monitoring." *IEEE Transactions on*  
773 *Geoscience and Remote Sensing* 48 (2): 852–863. doi:10.1109/TGRS.2009.2036253.

774 Kim, T.-S., K.-A. Park, L. Xiaofeng, M. Lee, S. Hong, S. J. Lyu, and S. Nam. 2015. "Detection of the Hebei Spirit Oil Spill on SAR Imagery  
775 and Its Temporal Evolution in a Coastal Region of the Yellow Sea." *Advances in Space Research* 56 (6): 1079–1093.  
776 doi:10.1016/j.asr.2015.05.040.

777 Konik, M., and K. Bradtke. 2016. "Object-Oriented Approach to  
778 Oil Spill Detection Using ENVISAT ASAR Images." *ISPRS Journal of Photogrammetry and Remote Sensing*  
779 118 (August): 37–52. doi:10.1016/j.isprsjprs.2016.04.006.

780 Lang, H., X. Zhang, X. Yuyang, X. Zhang, and L. Wei. 2017. "Dark- Spot Segmentation for Oil Spill Detection Based on Multifeature Fusion  
781 Classification in Single-Pol Synthetic Aperture Radar Imagery." *Journal of Applied Remote Sensing* 11 (January): 015006.  
782 doi:10.1117/1.JRS.11.015006.

783 Latini, D., D. F. Fabio, and C. E. Jones. 2016. "Multi-Frequency and Polarimetric Quantitative Analysis of the Gulf of Mexico  
784 Oil Spill Event Comparing Different SAR Systems." *Remote Sensing of Environment* 183 (September): 26–42.  
785 doi:10.1016/j.rse.2016.05.014.

786 Lee, J. S., L. Jurkevich, P. Dewaele, P. Wambacq, and A. Oosterlinck. 1994. "Speckle Filtering of Synthetic Aperture Radar Images: A  
787 Review." *Remote Sensing Reviews* 8 (4): 313–340. doi:10.1080/02757259409532206. Taylor & Francis.

788 Leifer, I., W. J. Lehr, D. Simecek-Beatty, E. Bradley, R. Clark, P. Dennison, H. Yongxiang, et al. 2012. "State of the Art Satellite and Airborne  
789 Marine Oil Spill Remote Sensing:  
790 Application to the BP Deepwater Horizon Oil Spill." *Remote Sensing of Environment* 124 (September): 185–209.  
791 doi:10.1016/j.rse.2012.03.024.

792 Li, G., L. Ying, B. Liu, W. Peng, and C. Chen. 2019. "Marine Oil Slick Detection Based on Multi-Polarimetric Features Matching Method  
793 Using Polarimetric Synthetic Aperture Radar Data." *Sensors* 19 (23): 5176. doi:10.3390/s19235176. Multidisciplinary Digital  
794 Publishing Institute.

795 Li, X., L. Chunyan, Z. Yang, and W. Pichel. 2013. "SAR Imaging of Ocean Surface Oil Seep Trajectories Induced by near Inertial Oscillation."  
796 *Remote Sensing of Environment* 130 (March): 182–187. doi:10.1016/j.rse.2012.11.019.

797 Li, X., T. Jia, and D. Velotto. 2016a. "Spatial and Temporal Variations of Oil Spills in the North Sea Observed by the Satellite Constellation  
798 of TerraSAR-X and TanDEM-X." *IEEE Journal of Selected Topics in Applied Earth Observations and Remote Sensing* 9 (11): 4941–4947.  
799 doi:10.1109/JSTARS.2016.2519444.

800 Li, X., T. Jia, and D. Velotto. 2016b. "Spatial and Temporal Variations of Oil Spills in the North Sea Observed by the Satellite Constellation  
801 of TerraSAR-X and TanDEM-X." *IEEE Journal of Selected Topics in Applied Earth Observations and Remote Sensing* 9 (11): 4941–4947.  
802 doi:10.1109/JSTARS.2016.2519444.

803 Li, Y., Y. Zhang, Z. Yuan, H. Guo, H. Pan, and J. Guo. 2018. "Marine Oil Spill Detection Based on the Comprehensive Use of Polarimetric  
804 SAR Data." *Sustainability* 10 (12): 4408. doi:10.3390/su10124408. Multidisciplinary Digital  
805 Publishing Institute.

806 Liu, P., C. Zhao, L. Xiaofeng, H. Mingxia, and W. Pichel. 2010. "Identification of Ocean Oil Spills in SAR Imagery Based on  
807 Fuzzy Logic Algorithm." *International Journal of Remote Sensing* 31 (September): 4819–4833. doi:10.1080/01431161.2010.485147.

808 Loew, A., and W. Mauser. 2007. "Generation of Geometrically and Radiometrically Terrain Corrected SAR Image Products." *Remote*  
809 *Sensing of Environment* 106 (3): 337–349. doi:10.1016/j.rse.2006.09.002.

810 Lupidi, A., D. Staglianò, M. Martorella, and F. Berizzi. 2017. "Fast Detection of Oil Spills and Ships Using SAR Images." *Remote Sensing* 9  
811 (3): 230. doi:10.3390/rs9030230. Multidisciplinary Digital Publishing Institute.

812 MacDonald, I. R., O. Garcia-Pineda, A. Beet, S. Daneshgar Asl, L. Feng, G. Graettinger, D. French-mccay, et al. 2015. "Natural and  
813 Unnatural Oil Slicks in the Gulf of Mexico." *Journal of Geophysical Research (Oceans)* 120 (December): 8364–8380.  
814 doi:10.1002/2015JC011062.

815 Mahdianpari, M., H. Jafarzadeh, J. E. Granger,  
816 F. Mohammadimanesh, B. Brisco, B. Salehi, S. Homayouni, and Q. Weng. 2020. "A Large-Scale Change Monitoring of Wetlands Using  
817 Time Series Landsat Imagery on Google  
818 Earth Engine: A Case Study in Newfoundland." *GIScience &*  
819 *Remote Sensing* 57 (8): 1102–1124. doi:10.1080/15481603.2020.1846948. Taylor & Francis.

820 Marghany, M. 2016. "Automatic Mexico Gulf Oil Spill Detection from Radarsat-2 SAR Satellite Data Using Genetic Algorithm." *Acta*  
821 *Geophysica* 64 (5): 1916–1941. doi:10.1515/acgeo-2016-0047.

822 Martinis, S., M. Gähler, and A. Twele. 2012. "A Multi-Scale Markov Model for Unsupervised Oil Spill Detection in  
823 TerraSAR-X Data." In *2012 IEEE International Geoscience and Remote Sensing Symposium*, Munich, Germany 923–926.  
824 doi:10.1109/IGARSS.2012.6351405.

825 Marzialetti, P., and G. Laneve. 2016. "Oil Spill Monitoring on Water Surfaces by Radar L, C and X Band SAR Imagery: A Comparison of  
826 Relevant Characteristics." In *2016 IEEE International Geoscience and Remote Sensing Symposium (IGARSS)*, Beijing, China, 7715–  
827 7717. doi:10.1109/IGARSS.2016.7731012.

828 McCandless, S. W., and C. R. Jackson. 2004. "Principles of Synthetic Aperture Radar." In *Synthetic Aperture Radar Marine User's Manual*,  
829 1–24. Washington, DC: US Dept. of Commerce NOAA/NESDIS Publication, US Govt. Print. Office.

830 Mera, D., J. M. Cotos, J. Varela-Pet, and O. Garcia-Pineda. 2012. "Adaptive Thresholding Algorithm Based on SAR Images and Wind Data  
831 to Segment Oil Spills along the Northwest Coast of the Iberian Peninsula." *Marine Pollution Bulletin* 64 (10): 2090–2096.  
832 doi:10.1016/j.marpolbul.2012.07.018.

833 Mera, D., J. M. Cotos, J. Varela-Pet, P. G. Rodríguez, and A. Caro. 2014. "Automatic Decision Support System Based on SAR Data for Oil  
834 Spill Detection." *Computers & Geosciences* 72 (November): 184–191. doi:10.1016/j.cageo.2014.07.015.

835 Mera, D., V. Bolon-Canedo, J. M. Cotos, and A. Alonso-Betanzos. 2017. "On the Use of Feature Selection to Improve the Detection of  
836 Sea Oil Spills in SAR Images." *Computers & Geosciences* 100 (March): 166–178. doi:10.1016/j.cageo.2016.12.013.

837 Mercier, G., and F. Arduin. 2006a. "Partially Supervised Oil-Slick Detection by SAR Imagery Using Kernel Expansion." *IEEE Transactions*  
838 *on Geoscience and Remote Sensing* 44 (10): 2839–2846. doi:10.1109/TGRS.2006.881078. IEEE Geoscience and Remote Sensing  
839 Society.

840 Mercier, G., and F. Arduin. 2006b. "Partially Supervised Oil-Slick Detection by SAR Imagery Using Kernel Expansion." *IEEE Transactions*  
841 *on Geoscience and Remote Sensing* 44 (10): 2839–2846. doi:10.1109/TGRS.2006.881078. IEEE Geoscience and Remote Sensing  
842 Society.

843 Mercier, G., and F. Girard-Arduin. 2005. "Unsupervised Oil Slick Detection by SAR Imagery Using Kernel Expansion." In *Proceedings.*  
844 *2005 IEEE International Geoscience and Remote*  
845 *Sensing Symposium, 2005. IGARSS '05., Seoul, Korea (South), 1:4.* doi:10.1109/IGARSS.2005.1526219.

846 Mercier, G., S. Derrode, W. Pieczynski, J. Le Caillec, and R. Garello. 2003. "Multiscale Oil Slick Segmentation with Markov Chain Model."  
847 In *IGARSS 2003. 2003 IEEE International Geoscience and Remote Sensing Symposium. Proceedings (IEEE Cat. No.03CH37477)*,  
848 Toulouse, France, 6: 3501–3503. doi:10.1109/IGARSS.2003.1294834.

849 Migliaccio, M., F. Nunziata, and A. Buono. 2015. "SAR Polarimetry for Sea Oil Slick Observation." <https://pubag.nal.usda.gov/catalog/2857224>  
850

851 Migliaccio, M., G. Ferrara, A. Gambardella, F. Nunziata, and A. Sorrentino. 2007. "A Physically Consistent Stochastic Model to Observe  
852 Oil Spills and Strong Scatterers on SLC SAR Images." In *2007 IEEE International Geoscience and Remote Sensing Symposium*,  
853 Barcelona, Spain, 1322–1325. doi:10.1109/IGARSS.2007.4423049.

854 Mihoub, Z., and A. Hassini. 2014. "Monitoring and Identification of Marine Oil Spills Using Advanced Synthetic Aperture Radar Images."  
855 *Optica Applicata* 44 (nr): 3. doi:10.5277/oa140308.

856 Minchew, B., C. E. Jones, and B. Holt. 2012. "Polarimetric Analysis of Backscatter from the Deepwater Horizon Oil Spill Using L-Band  
857 Synthetic Aperture Radar." *IEEE Transactions on Geoscience and Remote Sensing* 50 (10): 3812–3830.  
858 doi:10.1109/TGRS.2012.2185804.

859 Misra, A., and R. Balaji. 2017. "Simple Approaches to Oil Spill Detection Using Sentinel Application Platform (Snap)-ocean Application  
860 Tools and Texture Analysis: A Comparative Study." *Journal of the Indian Society of Remote Sensing* 45 (6): 1065–1075.  
861 doi:10.1007/s12524-016-0658-2.

862 Moher, D., A. Liberati, J. Tetzlaff, and D. G. Altman. 2009. "Preferred Reporting Items for Systematic Reviews and Meta-Analyses: The  
863 PRISMA Statement." *Annals of Internal Medicine* 151 (4): 264–269. doi:10.7326/0003-4819-151-4-200908180-00135. American  
864 College of  
865 Physicians.

866 Montali, A., G. Giacinto, M. Migliaccio, and A. Gambardella. 2006. "Supervised Pattern Classification Techniques for Oil Spill  
867 Classification in SAR Images: Preliminary Results." SEASAR 2006 Workshop, ESA-ESRIN, Frascati, Italy, 23–26 January.

868 Moreira, A., P. Prats-Iraola, M. Younis, G. Krieger, I. Hajnsek, and K. P. Papathanassiou. 2013. "A Tutorial on Synthetic Aperture Radar."  
869 *IEEE Geoscience and Remote Sensing Magazine* 1 (1): 6–43. doi:10.1109/MGRS.2013.2248301.

870 Najoui, Z., S. Riazanoff, B. Deffontaines, and J.-P. Xavier. 2018. "A Statistical Approach to Preprocess and Enhance C-Band SAR Images  
871 in order to Detect Automatically Marine Oil Slicks." *IEEE Transactions on Geoscience and Remote Sensing* 56 (5): 2554–2564.  
872 doi:10.1109/TGRS.2017.2760516.

873 Nunziata, F., A. Buono, and M. Migliaccio. 2018. "COSMO– SkyMed Synthetic Aperture Radar Data to Observe the Deepwater Horizon  
874 Oil Spill." *Sustainability* 10 (10): 3599. doi:10.3390/su10103599. Multidisciplinary Digital  
875 Publishing Institute.

876 Nunziata, F., A. Gambardella, and M. Migliaccio. 2008. "On the Mueller Scattering Matrix for SAR Sea Oil Slick Observation." *IEEE*  
877 *Geoscience and Remote Sensing Letters* 5 (4): 691–695. doi:10.1109/LGRS.2008.2003127.

878 Nunziata, F., A. Gambardella, and M. Migliaccio. 2013. "On the Degree of Polarization for SAR Sea Oil Slick Observation."  
879 *ISPRS Journal of Photogrammetry and Remote Sensing*  
880 78 (April): 41–49. doi:10.1016/j.isprsjprs.2012.12.007.

881 Nunziata, F., C. R. de Macedo, A. Buono, D. Velotto, and M. Migliaccio. 2019. "On the Analysis of a Time Series of X-Band TerraSAR-X  
882 SAR Imagery over Oil Seepages." *International Journal of Remote Sensing* 40 (May): 3623–3646.  
883 doi:10.1080/01431161.2018.1547933.

884 O'Rourke, D., and S. Connolly. 2003. "Just Oil? The Distribution of Environmental and Social Impacts of Oil Production and  
885 Consumption." *Annual Review of Environment and Resources* 28 (1): 587–617. doi:10.1146/annurev.energy.28.050302.105617.

886 Ozkan, C., B. Osmanoglu, F. Sunar, G. Staples, K. Kalkan, and F. Balik Sanli. 2012. "Testing the Generalization Efficiency of Oil Slick  
887 Classification Algorithm Using Multiple SAR Data for Deepwater Horizon Oil Spill." *ISPRS - International Archives of the  
888 Photogrammetry, Remote Sensing and Spatial Information Sciences* 39B7 (July): 67–72. doi:10.5194/isprsarchives-XXXIX- B7-67-  
889 2012.

890 Pelizzari, S., and J. Bioucas-Dias. 2007. "Oil Spill Segmentation of SAR Images via Graph Cuts." In *2007 IEEE International Geoscience and  
891 Remote Sensing Symposium, Barcelona, Spain*. doi:10.1109/IGARSS.2007.4423048.

892 Perkovic, M., H. Greidanus, O. Müllenhoff, G. Ferraro, P. Pavlakis, S. Cosoli, and R. Harsch. 2010. "Marine Polluter Identification:  
893 Backtracking with the Aid of Satellite Imaging." *Fresenius Environmental Bulletin* 19 (10b): 2426–2432. Parlar Scientific Publications.

894 Quintero-Marmol, A. M., E. C. Pedroso, C. H. Beisl, R. G. Caceres, F. P. De Miranda, K. Bannerman, P. Welgan, and O. L. Castillo. 2003.  
895 "Operational Applications of RADARSAT-1 for the Monitoring of Natural Oil Seeps in the South Gulf of Mexico." In *IGARSS 2003. 2003  
896 IEEE International Geoscience and Remote Sensing Symposium. Proceedings (IEEE Cat. No.03CH37477)*, Toulouse, France, 4: 2744–  
897 2746. doi:10.1109/IGARSS.2003.1294571.

898 Raeisi, A., G. Akbarizadeh, and A. Mahmoudi. 2018. "Combined Method of an Efficient Cuckoo Search Algorithm and Nonnegative Matrix  
899 Factorization of Different Zernike Moment Features for Discrimination between Oil Spills and  
900 Lookalikes in SAR Images." *IEEE Journal of Selected Topics in  
901 Applied Earth Observations and Remote Sensing*  
902 11 (November): 4193–4205. doi:10.1109/  
903 JSTARS.2018.2841503.

904 Robbe, N., and T. Hengstermann. 2006. "Remote Sensing of Marine Oil Spills from Airborne Platforms Using Multi-Sensor Systems." In  
905 *Water Pollution VIII: Modelling, Monitoring and Management*, Vol. 95, 347–355. Bologna, Italy: WIT Press. doi:10.2495/WP060351.

906 Salberg, A.-B., Ø. Rudjord, and A. H. Schistad Solberg. 2014. "Oil Spill Detection in Hybrid-Polarimetric SAR Images." *IEEE Transactions  
907 on Geoscience and Remote Sensing* 52 (10): 6521–6533. doi:10.1109/TGRS.2013.2297193.

908 Sefah-Twerefour, A. A., G. Wiafe, and K. Adu Agyekum. 2012. "Development OF an Algorithm for Automatic Detection OF Oil Slicks from  
909 Synthetic Aperture Radar (SAR) Imagery in the Gulf OF Guinea." In *2012 IEEE International Geoscience and Remote Sensing  
910 Symposium*, Munich, Germany, 2105–2108.  
911 doi:10.1109/IGARSS.2012.6351091.

912 Shah, P., T. Zaveri, R. Kumar, S. Sharma, and D. Patel. 2017. "Research Oriented Foss Solution for Automatic Oil Spill Detection Using  
913 Risat-1 Sar Data." In *2017 IEEE International Geoscience and Remote Sensing Symposium (IGARSS)*, Fort Worth, TX, 3121–3124.  
914 doi:10.1109/IGARSS.2017.8127659.

915 Shahsavarhighi, S., M. R. Sahebi, M. J. Valdanzoej, and  
916 G. Ataollah Haddadi. 2013. "A Comparison of IEM and SPM Model for Oil Spill Detection Using Inversion Technique and Radar Data."  *917 Journal of the Indian Society of Remote Sensing* 41 (2): 425–431. doi:10.1007/s12524- 012-0217-4.

918 Shao, W., Y. Sheng, and J. Sun. 2017. "Preliminary Assessment of Wind and Wave Retrieval from Chinese Gaofen-3 SAR Imagery."  *919 Sensors* 17 (8): 1705. doi:10.3390/s17081705. Multidisciplinary Digital Publishing Institute.

920 Shao, Y., W. Tian, S. Wang, and F. Zhang. 2008. "Oil Spill Monitoring Using Multi-Temporal SAR and Microwave Scatterometer Data." In  
921 *IGARSS 2008-2008 IEEE International Geoscience and Remote Sensing Symposium*, Boston, MA, USA, 3: III-1378-III-1381.  
922 doi:10.1109/IGARSS.2008.4779617.

923 Sharafat, G. 2000. "Towards the Development of an  
924 Operational Strategy for Oil Spill Detection and Monitoring in the Caspian Sea Based upon a Technical Evaluation of Satellite Sar  
925 Observations in Southeast Asia." *ISPRS - International Archives of the Photogrammetry, Remote Sensing and Spatial Information  
926 Sciences* 33: 295–299.1.

927 Shirvany, R., M. Chabert, and J.-Y. Tournet. 2012. "Ship and Oil-Spill Detection Using the Degree of Polarization in Linear and  
928 Hybrid/Compact Dual-Pol SAR." *IEEE Journal of Selected Topics in Applied Earth Observations and Remote Sensing* 5 (3): 885–892.  
929 doi:10.1109/JSTARS.2012.2182760.

930 Shu, Y., L. Jonathan, H. Yousif, and G. Gomes. 2010. "Dark-Spot Detection from SAR Intensity Imagery with Spatial Density  
931 Thresholding for Oil-Spill Monitoring." *Remote Sensing of Environment* 114 (9): 2026–2035. doi:10.1016/j. rse.2010.04.009.

932 Singha, S., M. Vespe, and O. Trieschmann. 2013. "Automatic Synthetic Aperture Radar Based Oil Spill Detection and Performance  
933 Estimation via a Semi-Automatic Operational Service Benchmark." *Marine Pollution Bulletin* 73 (1): 199–209.  
934 doi:10.1016/j.marpolbul.2013.05.022.

935 Singha, S., R. Ressel, D. Velotto, and S. Lehner. 2016. "A Combination of Traditional and Polarimetric Features for Oil Spill Detection  
936 Using TerraSAR-X." *IEEE Journal of Selected  
937 Topics in Applied Earth Observations and Remote Sensing* 9 (11): 4979–4990. doi:10.1109/JSTARS.2016.2559946.

938 Singha, S., T. J. Bellerby, and O. Trieschmann. 2012. "Detection and Classification of Oil Spill and Look-Alike Spots from SAR Imagery  
939 Using an Artificial Neural Network." In *2012 IEEE*

940 *International Geoscience and Remote Sensing Symposium,*  
941 Munich, Germany, 5630–5633. doi:10.1109/  
942 IGARSS.2012.6352042.

943 Skrunes, S., C. Brekke, C. E. Jones, M. M. Espeseth, and B. Holt. 2018. “Effect of Wind Direction and Incidence Angle on Polarimetric SAR  
944 Observations of Slicked and Unslicked Sea Surfaces.” *Remote Sensing of Environment* 213 (August): 73–91.  
945 doi:10.1016/j.rse.2018.05.001.

946 Skrunes, S., C. Brekke, and T. Eltoft. 2014. “Characterization of Marine Surface Slicks by Radarsat-2 Multipolarization Features.” *IEEE  
947 Transactions on Geoscience and Remote Sensing* 52 (9): 5302–5319. doi:10.1109/TGRS.2013.2287916.

948 Skrunes, S., C. Brekke, T. Eltoft, and V. Kudryavtsev. 2015. “Comparing Near-Coincident C- and X-Band SAR  
949 Acquisitions of Marine Oil Spills.” *IEEE Transactions on Geoscience and Remote Sensing* 53 (4): 1958–1975.  
950 doi:10.1109/TGRS.2014.2351417.

951 Solberg, A. H. S. 2012. “Remote Sensing of Ocean Oil-Spill Pollution.” *Proceedings of the IEEE* 100 (10): 2931–2945.  
952 doi:10.1109/JPROC.2012.2196250.

953 Solberg, A. H. S., C. Brekke, and P. O. Husoy. 2007. “Oil Spill Detection in Radarsat and Envisat SAR Images.” *IEEE Transactions on  
954 Geoscience and Remote Sensing* 45 (3): 746–755. doi:10.1109/TGRS.2006.887019.

955 Song, D., B. Wang, W. Chen, N. Wang, S. Yu, Y. Ding, B. Liu, Z. Zhen, M. Xu, and T. Zhang. 2018. “An Efficient Marine Oil Spillage  
956 Identification Scheme Based on an Improved Active Contour Model Using Fully Polarimetric SAR Imagery.” *IEEE Access* 6: 67959–  
957 67981. doi:10.1109/ACCESS.2018.2876173.

958 Song, D., Y. Ding, L. Xiaofeng, B. Zhang, and X. Mingyu. 2017. “Ocean Oil Spill Classification with RADARSAT-2 SAR Based on an Optimized  
959 Wavelet Neural Network.” *Remote Sensing* 9 (8): 799. doi:10.3390/rs9080799. Multidisciplinary Digital Publishing Institute.

960 Stussi, N., T. C. Amélie Beaudoin, and P. Gigord. 1996. “Radiometric Correction of Multi-Configuration Spaceborne SAR Data over Hilly  
961 Terrain.” 457. <https://hal.inrae.fr/hal-02575756>

962 Sun, S., H. Chuanmin, G. A. Lian Feng, J. H. Swayze, G. Graettinger, I. MacDonald, O. Garcia, and I. Leifer. 2016. “Oil Slick Morphology  
963 Derived from AVIRIS Measurements of the Deepwater Horizon Oil Spill: Implications for Spatial Resolution Requirements of Remote  
964 Sensors.” *Marine Pollution Bulletin* 103 (1): 276–285. doi:10.1016/j.  
965 marpolbul.2015.12.003.

966 Temitope Yekeen, S., A. Balogun, and K. B. Wan Yusof. 2020. “A Novel Deep Learning Instance Segmentation Model for Automated  
967 Marine Oil Spill Detection.” *ISPRS Journal of  
968 Photogrammetry and Remote Sensing* 167 (September): 190–200. doi:10.1016/j.isprs.2020.07.011.

969 Tian, S., X. Huang, and L. Hongga. 2017. “A New Method to Calibrate Lagrangian Model with ASAR Images for Oil Slick Trajectory.”  
970 *Marine Pollution Bulletin* 116 (1): 95–102. doi:10.1016/j.marpolbul.2016.12.054.

971 Tong, S., X. Liu, Q. Chen, Z. Zhang, and G. Xie. 2019. “Multi-Feature Based Ocean Oil Spill Detection for Polarimetric SAR Data Using  
972 Random Forest and the Self-Similarity Parameter.” *Remote Sensing* 11 (4): 451. doi:10.3390/rs11040451. Multidisciplinary Digital  
973 Publishing Institute.

974 Topouzelis, K., A. Bernardini, G. Ferraro, S. Meyer-Roux, and D. Tarchi. 2006. “Satellite Mapping of Oil Spills in the Mediterranean Sea.”  
975 *Fresenius Environmental Bulletin* 15 (9): 1009–1014.

976 Topouzelis, K., and A. Pysillos. 2012. “Oil Spill Feature Selection and Classification Using Decision Tree Forest on SAR Image Data.”  
977 *ISPRS Journal of Photogrammetry and Remote Sensing* 68 (March): 135–143. doi:10.1016/j.isprs.2012.01.005.

978 Topouzelis, K., D. Stathakis, and V. Karathanassi. 2009. “Investigation of Genetic Algorithms Contribution to Feature Selection for Oil  
979 Spill Detection.” *International Journal of Remote Sensing* 30 (3): 611–625. doi:10.1080/01431160802339456. Taylor & Francis.

980 Topouzelis, K., V. Karathanassi, P. Pavlakis, and D. Rokos. 2007. “Detection and Discrimination between Oil Spills and Look-Alike  
981 Phenomena through Neural Networks.” *ISPRS  
982 Journal of Photogrammetry and Remote Sensing* 62 (4): 264–270. doi:10.1016/j.isprs.2007.05.003.

983 Topouzelis, K. N. 2008. “Oil Spill Detection by SAR Images: Dark Formation Detection, Feature Extraction and Classification Algorithms.”  
984 *Sensors* 8 (10): 6642–6659. doi:10.3390/s8106642. Molecular Diversity Preservation International.

985 Valenzuela, G. R. 1978. “Theories for the Interaction of Electromagnetic and Oceanic Waves — A Review.” *Boundary-Layer Meteorology*  
986 13 (1): 61–85. doi:10.1007/BF00913863.

987 Vanjare, A. C., S. Arvind, S. N. Omkar, J. Kishore, and V. Kumar. 2019. “GEP Algorithm for Oil Spill Detection and Differentiation from  
988 Lookalikes in RISAT SAR Images.” In *Soft Computing for Problem Solving*, edited by J. C. Bansal, K. N. Das, A. Nagar, K. Deep, and A. K.  
989 Ojha, 435–446. Advances in Intelligent Systems and Computing. Singapore: Springer. doi:10.1007/978-981-13-1592-3\_34.

990 Velotto, D., M. Migliaccio, F. Nunziata, and S. Lehner. 2011. “Dual-Polarized TerraSAR-X Data for Oil-Spill Observation.” *IEEE  
991 Transactions on Geoscience and Remote Sensing* 49 (12): 4751–4762. doi:10.1109/TGRS.2011.2162960.

992 Velotto, D., M. Soccorsi, and S. Lehner. 2014. “Azimuth Ambiguities Removal for Ship Detection Using Full Polarimetric X-Band SAR  
993 Data.” *IEEE Transactions on Geoscience and Remote Sensing* 52 (1): 76–88. doi:10.1109/TGRS.2012.2236337.

994 Vespe, M., G. Ferraro, M. Posada, H. Greidanus, and M. Perkovic. 2011. “Oil Spill Detection Using COSMO-SkyMed over the Adriatic  
995 Sea: The Operational Potential.” In *2011 IEEE*

996 *International Geoscience and Remote Sensing Symposium*, Vancouver, BC, Canada, 4403–4406. doi:10.1109/  
997 IGARSS.2011.6050208.

998 Vespe, M., and H. Greidanus. 2012. "SAR Image Quality Assessment and Indicators for Vessel and Oil Spill  
999 Detection." *IEEE Transactions on Geoscience and Remote*  
1000 *Sensing* 50 (11): 4726–4734. doi:10.1109/  
1001 TGRS.2012.2190293.

1002 Vijayakumar, and Rukmini. 2016. "A Neural Network Classification Approach For Oil Spill Detection On Sar  
1003 Images." [https://www.semanticscholar.org/paper/  
1004 A-NEURAL-NETWORK-CLASSIFICATION-APPROACH-FOR-OIL  
1005 -ON-Vijayakumar.-Rukmini  
1006 /d98adceb707f5ab86e2173ad5ea6ed036cfb4bc2](https://www.semanticscholar.org/paper/A-NEURAL-NETWORK-CLASSIFICATION-APPROACH-FOR-OIL-ON-Vijayakumar.-Rukmini/d98adceb707f5ab86e2173ad5ea6ed036cfb4bc2)

1007 Wang, P., H. Zhang, and V. M. Patel. 2017. "SAR Image Despeckling Using a Convolutional Neural Network." *IEEE Signal Processing*  
1008 *Letters* 24 (12): 1763–1767. doi:10.1109/LSP.2017.2758203.

1009 Wang, S., F. Xingyu, Y. Zhao, and H. Wang. 2015. "Modification of CFAR Algorithm for Oil Spill Detection from SAR Data." *Intelligent*  
1010 *Automation & Soft Computing* 21 (2): 163–174. doi:10.1080/10798587.2014.960228.

1011 Wang, X., Y. Shao, F. Zhang, and W. Tian. 2019. "Comparison of C- and L-Band Simulated Compact Polarized SAR in Oil Spill Detection." *Frontiers of Earth Science* 13 (June): 351–360.  
1012 doi:10.1007/s11707-018-0733-9.

1013 Wismann, V., M. Gade, W. Alpers, and H. Huhnerfuss. 1998. "Radar Signatures of Marine Mineral Oil Spills Measured by an Airborne  
1014 Multi-Frequency Radar." *International Journal of Remote Sensing* 19 (18): 3607–3623. doi:10.1080/014311698213849. Taylor &  
1015 Francis.

1016 Xing, Q., L. Lin, M. Lou, L. Bing, R. Zhao, and L. Zhenbo. 2015. "Observation of Oil Spills through Landsat Thermal Infrared Imagery: A  
1017 Case of Deepwater Horizon." *Aquatic Procedia, Maritime Oil Spill Response* 3 (March): 151–156. doi:10.1016/j.aqpro.2015.02.205.

1018 Xu, L., L. Jonathan, and A. Brenning. 2014. "A Comparative Study of Different Classification Techniques for Marine Oil Spill  
1019 Identification Using RADARSAT-1 Imagery." *Remote Sensing of Environment* 141 (February): 14–23. doi:10.1016/j.rse.2013.10.012.

1020 Xu, L. M., J. Shafiee, A. Wong, L. Fan, L. Wang, and D. Clausi. 2015. "Oil Spill Candidate Detection from SAR Imagery Using a  
1021 Thresholding-Guided Stochastic Fully-Connected Conditional Random Field Model." In *2015 IEEE Conference on Computer Vision*  
1022 *and Pattern Recognition Workshops (CVPRW)*, Boston, MA, USA, 79–86. doi:10.1109/CVPRW.2015.7301386.

1023 Yang, Y., L. Ying, and X. Zhu. 2017. "A Novel Oil Spill Detection Method from Synthetic Aperture Radar Imageries via  
1024 A Bidimensional Empirical Mode Decomposition." *Acta Oceanologica Sinica* 36 (7): 86–94. doi:10.1007/s13131-017-1086-z.

1025 Yao, Q., Z. Q. Chang, X. M. Liu, L. Y. Zhang, and C. Zhao. 2014. "Analysis on Adaptability of Monitoring Methods for Oil Spill by Using SAR  
1026 Imagery." *Advanced Materials Research*. Trans Tech Publications Ltd.

1027 Yin, J., J. Yang, L. Zhou, and X. Liying. 2020. "Oil Spill Discrimination by Using General Compact Polarimetric SAR Features." *Remote*  
1028 *Sensing* 12 (3): 479. doi:10.3390/rs12030479. Multidisciplinary Digital Publishing Institute.

1029 Yin, J., W. Moon, and J. Yang. 2015. "Model-Based Pseudo-Quad-Pol Reconstruction from Compact  
1030 Polarimetry and Its Application to Oil-Spill Observation." *Research Article. Journal of Sensors* 2015: 1–8. Hindawi.  
1031 doi:10.1155/2015/734848.

1032 Yu, F., W. Sun, L. Jiaojiao, Y. Zhao, Y. Zhang, and G. Chen. 2017. "An Improved Otsu Method for Oil Spill Detection from SAR Images." *Oceanologia* 59 (3): 311–317. doi:10.1016/j.oceano.2017.03.005.

1033 Yu, X., H. Zhang, C. Luo, Q. Hairong, and P. Ren. 2018. "Oil Spill Segmentation via Adversarial  $\mathcal{F}$ -divergence Learning." *IEEE Transactions*  
1034 *on Geoscience and Remote Sensing* 56 (9): 4973–4988. doi:10.1109/TGRS.2018.2803038.

1035 Zeng, K., and Y. Wang. 2020. "A Deep Convolutional Neural Network for Oil Spill Detection from Spaceborne SAR Images." *Remote*  
1036 *Sensing* 12 (6): 1015. doi:10.3390/rs12061015. Multidisciplinary Digital Publishing Institute.

1037 Zhang, B., W. Perrie, L. Xiaofeng, and W. G. Pichel. 2011. "Mapping Sea Surface Oil Slicks Using RADARSAT-2 Quad-Polarization SAR  
1038 Image." *Geophysical Research Letters* 38 (May): L10602. doi:10.1029/2011GL047013.

1039 Zhang, F., Y. Shao, W. Tian, and S. Wang. 2008. "Oil Spill Identification Based on Textural Information of SAR Image." In *IGARSS 2008-*  
1040 *2008 IEEE International Geoscience and Remote Sensing Symposium*, Boston, MA, USA, 4: IV- 1308-IV–1311.  
1041 doi:10.1109/IGARSS.2008.4779971.

1042 Zhang, J., H. Feng, Q. Luo, L. Yu, J. Wei, and L. Jian. 2020. "Oil Spill Detection in Quad-Polarimetric SAR Images Using an Advanced  
1043 Convolutional Neural Network Based on SuperPixel Model." *Remote Sensing* 12 (March): 944. doi:10.3390/rs12060944.

1044 Zhang, Y., L. X. Yu, S. Liang, and J. Tsou. 2017. "Comparison of Oil Spill Classifications Using Fully and Compact Polarimetric SAR Images." *Applied Sciences* 7 (2): 193. doi:10.3390/app7020193. Multidisciplinary Digital Publishing Institute.

1045 Zhao, J., M. Temimi, H. Ghedira, and H. Chuanmin. 2014a. "Exploring the Potential of Optical Remote Sensing for Oil Spill Detection in  
1046 Shallow Coastal Waters-a Case Study in the Arabian Gulf." *Optics Express* 22 (June): 13755. doi:10.1364/OE.22.013755.

- 1050 Zhao, J., M. Temimi, H. Ghedira, and H. Chuanmin. 2014b. "Exploring the Potential of Optical Remote Sensing for Oil Spill Detection in  
1051 Shallow Coastal Waters-a Case Study in the Arabian Gulf." *Optics Express* 22 (11): 13755–13772. doi:10.1364/OE.22.013755. Optical  
1052 Society of America.
- 1053 Zheng, H., Y. Zhang, Y. Wang, X. Zhang, and J. Meng. 2017. "The Polarimetric Features of Oil Spills in Full Polarimetric Synthetic Aperture  
1054 Radar Images." *Acta Oceanologica Sinica* 36 (5): 105–114. doi:10.1007/s13131-017-1065-4.
- 1055 Zou, Y., L. Shi, S. Zhang, C. Liang, and T. Zeng. 2016. "Oil Spill  
1056 Detection by a Support Vector Machine Based on Polarization Decomposition Characteristics." *Acta Oceanologica Sinica* 35 (9): 86–  
1057 90. doi:10.1007/s13131-016-0935-5.